N69-38223
NASA CR-105975

The Application of Signal Detection Theory to Optics

PROGRESS REPORT

NASA Grant 05-009-079

September 15, 1969

Carl W. Helstrom

Department of Applied Physics and Information Science

University of California, San Diego

La Jolla, California 92037

ABSTRACT

Research undertaken during the quarter ending September 15, 1969, is outlined. Topics included are the use of a modal decomposition of the aperture field in the detection of incoherently radiating objects and the mapping of the radiance function of the object plane, mean-square errors in the estimation of radiance at sample points of the object plane, and the properties of filters and predictors involving the discrete Fourier transform.

1. Detection and Resolution of Incoherent Objects

Incoherently radiating objects produce at the aperture of an optical instrument an electromagnetic field that is best described as a spatio-temporal random process. Also present there is a background field of a similar kind, but with much broader distributions in frequency and angle. A telescope or other instrument that is to detect the presence of the object must process its aperture field in such a way that an observer can most surely decide whether the field contains a constituent due to the object or not.

This detection problem is similar to the problem of detecting a stochastic signal in white Gaussian noise, which has been treated by communication theory, and the same methods can be brought to bear on it. A particularly useful one is the Karhunen-Loève expansion in terms of the autocovariance function of the signal. In optical detection, the expansion functions are the eigenfunctions of a Fredholm integral equation whose kernel is the mutual coherence function of the light from the object. By counting the number of significantly large terms in the expansion, one can assess the number of degrees of freedom in the aperture field that contribute to detection of the object. The result gives a precise meaning to the related number of degrees of freedom in an image. For an extensive object the eigenvalues of the integral equation are proportional to samples of the radiance function of the object at points separated by a conventional resolution interval.

Furthermore, this modal decomposition of the aperture field permits deriving the optimum detector of the object when the quantum-mechanical properties of the light must be taken into account, and the performance of the optimum detector as a function of the characteristics of the object can be assessed. Mapping the radiance function of the object plane can be treated as an estimation problem from the same point of view.

Details of this research and its results are presented in a paper, "The Modal Decomposition of Aperture Fields in Detection and Estimation of Incoherent Objects", attached as an appendix to this report.

In analyzing the detectability of a uniformly radiating circular object, the eigenvalues associated with the generalized prolate spheroidal harmonics were needed. Various methods were investigated for computing them, among which was the application of the Rayleigh-Ritz method to the differential equation for those functions. In the course of this work some apparently new integral formulas involving the Legendre polynomials were discovered. They are presented in a brief paper, "Some Integrals Involving Legendre Polynomials", attached as an appendix to this report.

When a telescope or other optical instrument is used to resolve details in an object plane, what is in effect being done is to estimate the radiance function of that plane. It is generally recognized that details whose angular subtense is less than λ/a cannot easily be resolved, λ being the wavelength of the object light and $\underline{a}$ the diameter of the aperture of the instrument. This limitation can be more precisely formulated in terms of the mean-square errors incurred in estimates of samples of the radiance function at the points of a lattice superimposed on the object plane. It is shown that when the separation of the sampling points is reduced much below the size of a conventional resolution element, those mean-square errors become extremely large. Details of this matter are presented in an attachment to this report entitled "Resolution of Incoherent Objects from the Standpoint of Statistical Estimation Theory".

2. Discrete-Fourier-Transform Filters

(prepared by Charles L. Rino)

The purpose of this work is to evaluate the performance of certain discrete-Fourier-transform approximations to linear mean-square filters. These methods have been in use extensively since the development of the Cooley-Tukey fast Fourier-transform algorithm. In their application, however, they are interpreted as approximations to filters designed for continuously available or sampled data, and the increase in the mean-square error has been only qualitatively assessed. There is, of course, no serious difficulty in this approach. We can show, however, that with a slight modification of one standard approach we are led directly to the discrete transform filters.

Consider the jointly stationary random processes $\{Y_j\}$ and $\{Z_k\}$. We are interested in linear estimators of the form

$$\hat{Y}_{n-j} = \sum_{k \varepsilon J} M_{j,k} \, Z_{n-k} \tag{1}$$

where J is a set of integers describing the available data. Three cases are of interest. If J is the finite set of integers, say $J = \{\ell : \; 0 \leq \ell \leq M\}$, (1) can be written in vector form, and we have

$$\underset{\sim}{M}^{j} = \underset{\sim}{R}_{zz}^{-1} \, \underset{\sim}{R}^{1}{}_{yz} \tag{2}$$

where $\underset{\sim}{R}_{zz}$ is an $(M + 1) \times (M + 1)$ matrix with elements $[R_{zz}]_{i,j} = R_{zz_{i-j}}$, $\underset{\sim}{M}^{jT} = (M_{j,0}, M_{j,1}, \ldots, M_{j,M})$ and $\underset{\sim}{R}_{yz}^{j\,T} = (R_{yz_{-j}}, R_{yz_{1-j}}, \ldots, R_{yz_{M-j}})$. Equation (1) becomes

$$\hat{Y}_{n-j} = \underset{\sim}{M}^{jT} \, \underset{\sim}{Z} \tag{3}$$

with the mean-square error

$$||\varepsilon_j||^2 = E[(Y_{n-j} - \hat{Y}_{n-j})^2] = \underset{\sim}{R}_{yy}(0) - \underset{\sim}{R}_{yz}^{j\,T} R_{zz} \quad \underset{\sim}{R}_{yz}^{j}. \tag{4}$$

The covariance matrix is Toeplitz, and an efficient method is available for its inversion.[1] The method does, however, require M^2 operations, and the ensuing matrix operations are cumbrous. One would like to take advantage of the fact that $\underset{\sim}{R}_{zz}^{-1}$ itself is nearly Toeplitz. Hence for $|j - k| \ll M$, $[\underset{\sim}{R}_{zz}^{-1}]_{j,k}$ is approximately a function of $j - k$.[2] We can make use of this to avoid the matrix inversion in approximating $M_{j,k}$. The standard approach is to assume the data interval is infinite. Hence consider the following infinite-interval estimators.

If $J = \{\ell: -\infty < \ell < \infty\}$ we can use frequency-domain methods to derive the estimator

$$M_{j,k} = \int_{-\pi}^{\pi} m_j(\omega/\Delta x)\; e^{i\omega k} \frac{d\omega}{2\pi} \tag{5}$$

where

$$m_j(\omega/\Delta x) = \frac{e^{-i\omega j}\; \phi_{yz}(\omega/\Delta x)}{\phi_{zz}(\omega/\Delta x)} \tag{6}$$

In this case the filter $M_{j,k}$ is shift invariant, and it achieves a mean-square error

$$\varepsilon_\infty = ||\varepsilon_j||^2 = \int_{-\pi}^{\pi} [\phi_{yy}(\omega/\Delta x) - \frac{|\phi_{yz}(\omega/\Delta x)|^2}{\phi_{zz}(\omega/\Delta x)}] \frac{d\omega}{2\pi} \tag{7}$$

which is independent of j. We can now use the discrete Fourier transform to compute (4). We have

$$M_{p_{j,k}} = \frac{1}{N}\sum_{n=0}^{N-1} m_j\left(\frac{2\pi n}{N}\right) \; e^{2\pi i n k/N}, \tag{8}$$

where

$$M_{p_{j,k}} = \sum_{m=-\infty}^{\infty} M_{j,k+mN}. \tag{9}$$

---

1. W. F. Trench, J. Soc. Ind. Appl. Math., Vol. 12, pp. 515-522 (1969).
2. C. Rino, "Inversion of Covariance Matrices, IEEE Trans. Info. Theory, to appear March 1969.

For the class of spectra we are likely to encounter $m_j(\omega/\Delta x)$ will in the worst case contain jump discontinuities. Hence $M_{j,k}$ is $0(|k|^{-1})$, and the "alias" error

$$\varepsilon_A(\rho) = M_{j,\rho N} - M_{p_j,\rho N}, \tag{10}$$

for sufficiently large N, will be small for $|p| << N$. For a smooth function, i.e. one that has $2m + 2$ continuous derivatives, where $m > 1$, $\varepsilon_A(p)$ can be evaluated explicitly. The results are shown in Fig. 1.

From the preceding discussion we expect $M_{p_j,k}$ to achieve a mean-square error close to (7) except for j near the ends of the data interval. The increase in the mean-square error will be referred to as an end effect. We can verify this asymptotically. Consider

$$\begin{aligned} ||\varepsilon_j||^2 &= E[(Y_{n-j} - \hat{Y}_{n-j})^2] \\ &= E[Y_{n-j} - \hat{Y}^{\infty}_{n-j} + \hat{Y}^{\infty}_{n-j} - \hat{Y}_{n-j})^2] \\ &= \varepsilon^{\infty} + E[(\hat{Y}^{\infty}_{n-j} - \hat{Y}_{n-j})^2] \quad , \end{aligned} \tag{11}$$

since $E[\varepsilon_j(\hat{\underline{\underline{y}}}_{n-j} - \hat{\underline{\underline{y}}}_{n-j})] = 0$.

Here

$$\hat{Y}_{n-j} = \sum_{k=0}^{N-1} M_{p_j,k} Z_{n-k}$$

and

$$\hat{Y}^{\infty}_{n-j} = \sum_{k=-\infty}^{\infty} M_{j-k} Z_{n-k}.$$

The final term is asymptotically bounded above by $(M^{\infty}_{j-N} - M_{j-N})^2 R_{ZZ}(0) + 0(\frac{1}{N})$. Hence we have

$$||\varepsilon_j||^2 \lesssim \varepsilon_{\infty} + (\varepsilon_{A_{j-N}})^2 R_{ZZ}(0), \tag{12}$$

where the final term makes a large contribution near $j = 0$ and $j = N$.

Now consider the data set $J = \{\ell: \ell \leq 0\}$. In this case we must use the

Figure Caption

Alias Error vs. ρ For $f(\omega) = f^*(-\omega)$

$$\varepsilon_A(\rho) = \sum_{m=1}^{M} \frac{(-1)^m \Delta f_r^{(2m-1)}}{(N \times 10^{-1})^{2m}} F^e_{M,m}(\rho) - \sum_{m=1}^{M} \frac{(-1)^m \Delta f_r^{(2m-2)}}{(N \times 10^{-1})^{2m-1}} F^o_{M,m}(\rho) + E_M(\rho)$$

$$= \int_{-\pi}^{\pi} f(\omega/\Delta x)\; e^{i\omega k} \frac{d\omega}{2\pi} - \frac{1}{N}\sum_{n=0}^{N-1} f\left(\frac{2\pi n}{N}\right) e^{2\pi i n k/N}$$

$$\Delta f^{(k)} = f^{(k)}\;(\pi/\Delta x) - f^{(k)}\;(-\pi/\Delta x)$$

(Note: $F^o_{M,m}$ and $F^e_{M,m}$ are insensitive to the value of M for m << M.)

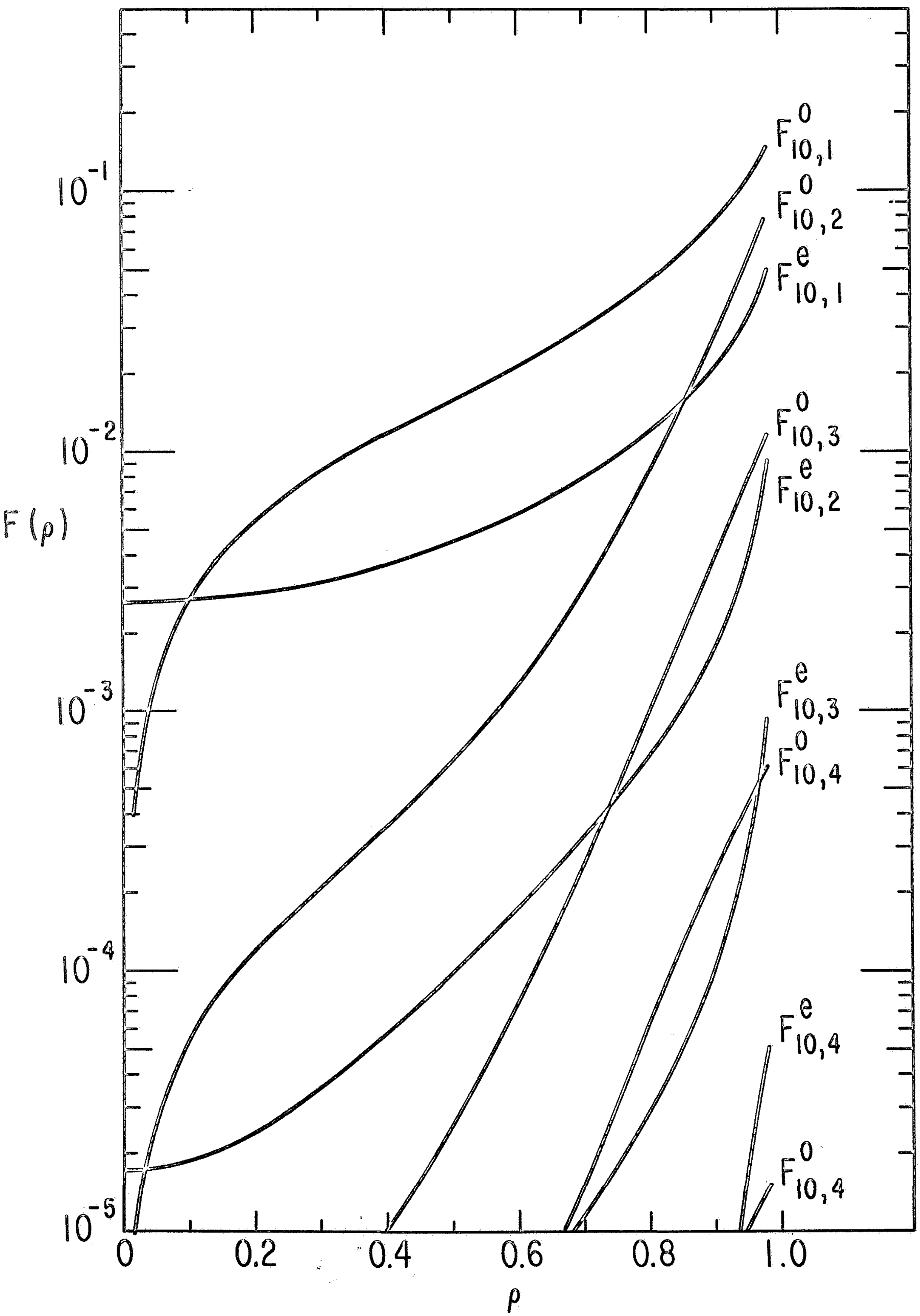

F (ρ)
10^-1
10^-2
10^-3
10^-4
10^-5
0
0.2
0.4
0.6
0.8
1.0
ρ
$F^0_{10,1}$
$F^0_{10,2}$
$F^e_{10,1}$
$F^0_{10,3}$
$F^e_{10,2}$
$F^e_{10,3}$
$F^0_{10,4}$
$F^e_{10,4}$
$F^0_{10,4}$

causal filter

$$m_j^{-\infty}(\omega/\Delta x) = \frac{1}{\phi_{zz}^{+}(\omega/\Delta x)}\left[\frac{e^{-i\omega j}\,\phi_{yz}(\omega/\Delta x)}{\phi_{zz}^{-}(\omega/\Delta x)}\right]_{+} \tag{13}$$

where the term in square brackets means

$$[e^{-i\omega j}\, f(\omega/\Delta x)]_{+} = \sum_{k=0}^{\infty} f_{k-j}\, e^{-i\omega k} \tag{14}$$

where $f(\omega/\Delta x) = \frac{\phi_{yz}(\omega/\Delta x)}{\phi_{zz}^{-}(\omega/\Delta x)}$ and f_k is the k-th Fourier coefficient of $f(\omega/\Delta x)$. The terms ϕ_{zz}^{+} and ϕ_{zz}^{-} constitute the canonical factorization of ϕ_{zz}. That is, $\phi_{zz} = \phi_{zz}^{+}\,\phi_{zz}^{-}$, and ϕ_{zz}^{+} has only positively indexed coefficients in its Fourier series; $\phi_{zz}^{-} = \phi_{zz}^{+*}$ has the opposite behavior. The filter achieves the j-dependent mean-square error

$$\varepsilon_j^{-\infty} = \int_{-\pi}^{\pi}\left[\phi_{yy}(\omega/\Delta x) - \frac{m_j^{-\infty}(\omega/\Delta x)\, e^{i\omega j}\,\phi_{yz}^{*}(\omega/\Delta x)}{\phi_{zz}(\omega/\Delta x)}\right]\frac{d\omega}{2\pi} \tag{15}$$

To approximate $m_j^{-\infty}(\omega/\Delta x)$ we must first factor ϕ_{zz}. It appears that $\phi_{zz}^{+}(\omega)$ can be evaluated exactly at $\omega = \frac{2\pi n}{N}$ for $-N/2 \le n \le N/2 - 1$. The details are currently being investigated. Computer tests have been encouraging, but some analytical questions remain. We have as yet found no method to evaluate (14) exactly. The problem stems from the fact that the positively indexed and negatively indexed coefficients become intermixed when the finite Fourier transform algorithm is applied. We have

$$a_{p_k} = \frac{1}{N}\sum_{n=0}^{N-1} f\left(\frac{2\pi n}{N}\right) e^{2\pi i nk/N} = a_{p_k}^{+} + a_{p_{N-k}}^{-} . \tag{16}$$

Since for large N $a_{p_k}^{+} \approx 0$ and $a_{p_{N-k}}^{-} \approx 0$ for k near N/2 and f sufficiently smooth, we can take

$$a^+_{p_k} \approx \begin{cases} a_{p_k} & k < N/2 \\ 0 & k \geq N/2. \end{cases} \qquad (17)$$

Good results have been obtained with this approximation for smooth spectra.

The approximation to (13) can be used to correct the end effect that (8) produces. In fact for large j (13) approaches (6), and the approximate filter can be used over the entire data interval except near $j = 0$, where the phase must be reversed. This is not efficient since (13) is much more difficult to evaluate than (6).

We indicated at the beginning that these methods can be formalized. The mean-square filter problem is usually formulated in an abstract Hilbert space with the covariance function serving as an inner product. If we use instead the inner product

$$\langle x_j, y_k \rangle = \sum_{m=-\infty}^{\infty} R_{xy_{k-j+mN}} \qquad (18)$$

we will be led directly to estimators of the form (6). In this case we are not minimizing the mean-square error, but the "p-norm" error, where the p-norm derived from (18) is $\langle x_j, x_j \rangle^{1/2}$. Similarly we can use a whitening approach. If we restrict the class of filters to those derived from functions with only positively indexed Fourier coefficients, we will be led to approximation of (13). The filters so derived are mean-square error filters for the class of circular random processes, which have been extensively analyzed.

Finally we will extend these methods to two dimensions. Certain fundamental difficulties arise since there is no general method for factoring multidimensional spectra. It can, however, be done for certain restricted classes of functions. We will also consider the fact that the covariances or spectra are never precisely known.

The Modal Decomposition of Aperture Fields
in Detection and Estimation of Incoherent Objects

Carl W. Helstrom
Department of Applied Physics and Information Science
University of California, San Diego; La Jolla, Calif. 92037

Abstract

A decomposition of the field at the aperture of an optical system in terms of the eigenfunctions of a certain integral equation is useful in analyzing the detectability of incoherent objects. The kernel of the integral equation is the mutual coherence function of the light from the object. The decomposition permits specification of the number of degrees of freedom in the aperture field contributing to detection of the object. Quantum-mechanically the coefficients of the modal decomposition become operators similar to the usual creation and annihilation operators for field modes. The optimum detector of the object is derived in terms of these operators. Specific detection probabilities are calculated for a uniform circular object whose light is observed at a circular aperture The modal decomposition is also applied to estimating the radiance distribution of the object plane.

Detection, resolution, and parameter estimation in the object space are the primary functions of an optical system. That space is usually taken to be a plane, the mapping of whose radiance distribution is an important type of parameter estimation. Detection and resolution, on the other hand, involve decisions among hypotheses about the object plane.[1,2]

The data upon which these decisions and estimates are based are the values of the electromagnetic field at the aperture A of the optical system, as observed during a finite interval (0, T). Lenses, stops, and photosensitive surfaces process the aperture field in such a way as to facilitate the decisions and estimates. The quality of the system can be measured by probabilities of correct decisions and mean-square errors in estimates of object parameters. These measures are instructively compared with the best values attainable by any system working with the same data. The ideal optical system that maximizes probabilities of correct decision or minimizes estimation errors is called the optimum system, and its structure can be determined by the methods of detection theory.[3,4]

When the object plane radiates incoherently, the analysis by detection theory employs a characteristic decomposition of the aperture field into spatial and temporal modes. The mode functions are the eigenfunctions of an integral equation whose kernel is the spatio-temporal mutual coherence function of the part of the aperture field generated by the object to be detected. The associated eigenvalues determine the detectability of the object through the probability distributions of the modal expansion coefficients. Generally only a finite number M_T of the eigenvalues are significantly different from zero, and only the field modes associated with them contribute substantially to detection. Thus M_T specifies the number of significant degrees of freedom in the aperture field relative to the detection of a certain object. For spectrally pure object light M_T can be factored into a number M of spatial degrees of freedom and a number M' of temporal degrees of freedom. The temporal factor M' is the product WT of the observation interval T and the bandwidth W of the object light.

When the light from the object possesses complete first-order coherence at the aperture, $M = 1$ and there is a single significant spatial mode. When the object is so large, on the other hand, that the coherence length of its light is much smaller than the diameter of the aperture, $M \gg 1$ and--as we shall see--the mode eigenvalues are proportional to values of the object radiance at sample points separated by a conventional resolution interval. If the aperture is provided with a lens to focus the light onto an image plane, each spatial mode, for $M \gg 1$, goes into a conventional resolution element of the image. Mapping the radiance of the object plane, furthermore, can be treated as estimating the eigenvalues of these spatial modes.

The eigenfunctions and eigenvalues of the mutual coherence function of the aperture field thus supply a precise meaning for the concept of informative degrees of freedom in the aperture field with respect to detection and resolution. There is a direct relation to the concept of degrees of freedom in an image, as treated by Toraldo di Francia and others.[5]

This paper will develop in some detail the modal decomposition of the aperture field and its application to the detection of an object and the estimation of the radiance distribution of the object plane. Associated with the spatio-temporal field modes are quantum-mechanical operators with much the same properties as the creation and annihilation operators in the usual form of field quantization.[6] Under normal conditions of observation, the operators for different modes commute, and the detection of an incoherent object can be based on the number of photons counted in each mode. Specific results are given for detecting a uniform circular object by observation of the field over a circular aperture.

The theory is developed for a scalar model of the electromagnetic field. Our results can be applied to ordinary unpolarized light by doubling the effective number M of spatial modes in the field at the aperture of the observing system.

I. The Modal Decomposition of the Aperture Field

The Field

In this section the electromagnetic field at the aperture will be treated classically, and for simplicity it will be taken as a scalar. The positive-frequency part of the field--or analytic signal--$\psi_+(\underset{\sim}{r}, t)$ is composed of a part $\psi_s(\underset{\sim}{r}, t)$ due to the object, when present, and a part $\psi_n(\underset{\sim}{r}, t)$ due to the background,

$$\psi_+(\underset{\sim}{r}, t) = \psi_s(\underset{\sim}{r}, t) + \psi_n(\underset{\sim}{r}, t). \tag{1.1}$$

The background field, or "noise", $\psi_n(\underset{\sim}{r}, t)$ is spatially and temporally white, its distribution being much broader in both frequency and direction than that of the object component, or "signal", $\psi_s(\underset{\sim}{r}, t)$.

Both signal and noise fields are circular-complex, spatio-temporal gaussian random processes.[7] The probability density functions describing them are specified completely by their mutual coherence functions

$$\tfrac{1}{2}\underset{\sim}{E}[\psi_n(\underset{\sim}{r}_1, t_1)\ \psi_n^*(\underset{\sim}{r}_2, t_2)] =$$

$$\varphi_n(\underset{\sim}{r}_1, t_1; \underset{\sim}{r}_2, t_2) = N'\delta(\underset{\sim}{r}_1 - \underset{\sim}{r}_2)\ \delta(t_1 - t_2), \tag{1.2}$$

$$\tfrac{1}{2}\underset{\sim}{E}[\psi_s(\underset{\sim}{r}_1, t_1)\ \psi_s^*(\underset{\sim}{r}_2, t_2)] = \varphi_s(\underset{\sim}{r}_1, t_1; \underset{\sim}{r}_2, t_2), \tag{1.3}$$

where $\underset{\sim}{E}$ stands for the statistical expectation and N' is the spatio-temporal spectral density of the background light. The mutual coherence function of the total field is $\varphi_n + \varphi_s$.

For convenience of discussion we assume the light from the object to be quasimonochromatic and spectrally pure, so that its mutual coherence function can be factored into spatial and temporal parts,

$$\varphi_s(\underset{\sim}{r}_1, t_1; \underset{\sim}{r}_2, t_2) = \varphi_s(\underset{\sim}{r}_1, \underset{\sim}{r}_2)\ \chi(t_1 - t_2)\ \exp i\Omega(t_1 - t_2), \tag{1.4}$$

where $\Omega = 2\pi c/\lambda$ is the central angular frequency of the object light, whose predominant wavelength is λ. The temporal autocovariance function $\chi(\tau)$ is normalized so that $\chi(0) = 1$, and the spatial part $\varphi_s(\underset{\sim}{r}_1, \underset{\sim}{r}_2)$--as in III--so that the illuminance at point $\underset{\sim}{r}$ of the aperture due to the object is $\varphi_s(\underset{\sim}{r}, \underset{\sim}{r})/2\Omega^2c$. The total energy received from the object during the interval (0, T) is

$$E_s = (2\Omega^2 c)^{-1} T \int_A \varphi_s(\underset{\sim}{r}, \underset{\sim}{r})\, d^2\underset{\sim}{r}.$$

The spectral density of the object light is

$$X(\omega) = \int_{-\infty}^{\infty} \chi(\tau)\, e^{i\omega\tau}\, d\tau, \tag{1.5}$$

with angular frequencies ω referred to Ω. Its bandwidth W is conveniently defined by

$$W = \left[\int_{-\infty}^{\infty} X(\omega)\, d\omega/2\pi\right]^2 \Bigg/ \int_{-\infty}^{\infty} [X(\omega)]^2\, d\omega/2\pi = |\chi(0)|^2 \Bigg/ \int_{-\infty}^{\infty} |\chi(\tau)|^2 d\tau. \tag{1.6}$$

We shall assume, as is normal in practice, that the observation time T is much greater than the correlation time W^{-1} of the object light; $WT \gg 1$.

The Modal Expansion

In treating the optimum detection of a temporal gaussian stochastic process, or random signal, in the presence of white noise, it is convenient to decompose the input to the receiver in a Karhunen-Loève expansion, whose terms are the eigenfunctions of the autocovariance function of the signal.[9] The coefficients of the expansion are statistically independent gaussian random variables in both the presence and the absence of the signal.

A similar expansion is useful in analyzing the detectability of optical fields.[10] The aperture field is written as

$$\psi_+(\underset{\sim}{r}, t) = \sum_p \sum_m a_{pm} f_{pm}(\underset{\sim}{r}, t), \tag{1.7}$$

where the a_{pm} are statistically independent gaussian random variables. The expansion functions $f_{pm}(\underset{\sim}{r}, t)$ are orthonormal over the aperture A and the interval (0, T),

$$\int_A \int_0^T f_{pm}{}^*(\underset{\sim}{r}, t) \, f_{qn}(\underset{\sim}{r}, t) \, d^2\underset{\sim}{r}dt = \delta_{pq} \, \delta_{mn}. \tag{1.8}$$

They are eigenfunctions of the integral equation

$$\lambda_{pm} \, f_{pm}(\underset{\sim}{r}, t) = C \int_A d^2\underset{\sim}{s} \int_0^T du \, \varphi_s(\underset{\sim}{r}, t; \underset{\sim}{s}, u) \, f_{pm}(\underset{\sim}{s}, u) \tag{1.9}$$

with C a suitable constant.

Because the object light is assumed spectrally pure, Eq. (1.4) permits us to break the eigenfunction $f_{pm}(\underset{\sim}{r}, t)$ into spatial and temporal factors,

$$f_{pm}(\underset{\sim}{r}, t) = \eta_p(\underset{\sim}{r}) \, \gamma_m(t) \, e^{-i\Omega t}, \tag{1.10}$$

$$\lambda_{pm} = h_p g_m, \tag{1.11}$$

where $\gamma_m(t)$ is an eigenfunction of $\chi(t - s)$,

$$g_m \gamma_m(t) = T^{-1} \int_0^T \chi(t - s)\, \gamma_m(s)\, ds \tag{1.12}$$

and $\eta_p(\underset{\sim}{r})$ an eigenfunction of $\varphi_s(\underset{\sim}{r}, \underset{\sim}{s})$,

$$h_p \eta_p(\underset{\sim}{r}) = (2\Omega^2 cT/E_s) \int_A \varphi_s(\underset{\sim}{r}, \underset{\sim}{s})\, \eta_p(\underset{\sim}{s})\, d^2\underset{\sim}{s}. \tag{1.13}$$

The constant C has been selected in such a way that Eq. (1.13) is equivalent to III, Eq. (5.6) with $h_p = \nu_p/N_s$, where N_s is the average total number of photons received from the object at the aperture A during the interval (0, T), and ν_p are the eigenvalues defined in III. Both sets of eigenfunctions sum to 1,

$$\sum_m g_m = 1, \qquad \sum_p h_p = 1, \tag{1.14}$$

and are considered as arranged in descending order.

The Temporal Integral Equation

Studying the temporal integral equation (1.12) briefly will help us understand the spatial one, Eq. (1.13). Since $WT \gg 1$, the width of the kernel $\chi(\tau)$ in Eq. (1.12) is much less than the length T of the interval of integration, and the spectral density $X(\omega)$ does not vary significantly as ω changes by $2\pi/T$. The eigenvalues are then approximately[11]

$$g_m \cong T^{-1} X(2\pi m/T), \quad m = \ldots -2, -1, 0, 1, 2, \ldots \tag{1.15}$$

The number of eigenvalues significantly different from zero is of the order of WT. The associated eigenfunctions are approximately the complex exponentials,

$$\gamma_m(t) \cong T^{-1/2} \exp(-2\pi i m t/T). \tag{1.16}$$

The highest frequencies appearing in the significant temporal modes, as measured with respect to $\Omega/2\pi$, are of the order of W.

If the autocovariance function $\chi(\tau)$ were periodic in τ with period T, the eigenvalues and eigenfunctions would be given exactly by the right-hand sides of Eqs. (1.15) and (1.16), as substitution into Eq. (1.12) easily demonstrates. When the width W^{-1} of $\chi(\tau)$ is much less than T, the fact that $\chi(\tau)$ is not periodic, but is concentrated about $\tau = 0$, does not alter g_m and $\gamma_m(t)$ very much.

Since we are mainly concerned here with the spatial properties of the aperture field, we shall assume that the temporal spectral density $X(\omega)$ is constant over the range $-\pi W < \omega < \pi W$ and zero elsewhere. There are then WT eigenvalues equal approximately to $(WT)^{-1}$, and all the temporal modes specified by the $\gamma_m(t)$ are equivalent. The exact eigenfunctions are the prolate spheroidal wavefunctions,[12] and the exact eigenvalues are nearly $g_m \equiv (WT)^{-1}$ for $1 \le |m| \le \frac{1}{2}WT$. The g_m become very small for $m > WT$. In optics the product WT may be 10^5 or more.

The Spatial Integral Equation

We suppose that the object to be detected is very far away and subtends a small solid angle from the point of observation. Its radiance is given by the function $B(\underset{\sim}{u})$, in which $\underset{\sim}{u}$ is a 2-vector of coordinates in the object plane. Then it follows from the Fresnel-Kirchhoff approximation that the spatial coherence function at the aperture is[13]

$$\varphi_S(\underset{\sim}{r}_1, \underset{\sim}{r}_2) = (8\pi R^2 \Omega^2 c)^{-1} \exp\left[\frac{ik}{2R}(\underset{\sim}{r}_1{}^2 - \underset{\sim}{r}_2{}^2)\right] \beta(\underset{\sim}{r}_2 - \underset{\sim}{r}_1), \qquad (1.17)$$

where $\beta(\underset{\sim}{r})$ is the Fourier transform of the object radiance,

$$\beta(\underset{\sim}{r}) = \int_O B(\underset{\sim}{u}) \exp(ik\underset{\sim}{u}\cdot\underset{\sim}{r}/R)\, d^2\underset{\sim}{u}. \qquad (1.18)$$

Here O indicates an integration over the object plane, R is the distance to the object, and $k = 2\pi/\lambda$.

By defining new eigenfunctions

$$\eta_p'(\underset{\sim}{r}) = \eta_p(\underset{\sim}{r}) \exp(-ik\underset{\sim}{r}^2/2R), \qquad (1.19)$$

we can write the spatial integral equation as

$$h_p \eta_p'(\underset{\sim}{r}_1) = [A\beta(0)]^{-1} \int_A \beta(\underset{\sim}{r}_2 - \underset{\sim}{r}_1)\, \eta_p'(\underset{\sim}{r}_2)\, d^2\underset{\sim}{r}_2, \qquad (1.20)$$

where A is the area of the aperture. The spatial integral equation has now the convolutional form of the temporal one, Eq. (1.12). The function $\beta(\underset{\sim}{r})$ corresponds to $\chi(\tau)$, the radiance $B(\underset{\sim}{u})$ to the spectal density $X(\omega)$.

When the object is a "point", that is, when it subtends from the aperture a solid angle much less than λ^2/A, the object field possesses first-order coherence over the aperture, $\beta(\underset{\sim}{r}) \equiv \beta(0)$. There is a single eigenvalue h_1 equal to 1, and the rest of the eigenvalues h_p are zero. The eigenfunction $\eta_1'(\underset{\sim}{r})$ associated with h_1 is constant, $\eta_1'(\underset{\sim}{r}) \equiv A^{-1/2}$. The remaining eigenfunctions can be an arbitrary set of functions orthonormal among themselves and to $\eta_1'(\underset{\sim}{r})$. Only a single field mode at the aperture is significant for detecting a point object or for estimating its radiance or its frequency.[14]

When the object is so large that its solid angle spans many multiples of λ^2/A, and when its radiance $B(\underset{\sim}{u})$ varies only slightly over distances of the order of $\lambda RA^{-\frac{1}{2}}$, the widths of the mutual coherence function and $\beta(\underset{\sim}{r})$ are much smaller than the diameter of the aperture. The eigenvalues h_p can then be approximated in the same manner as the g_m's in Eq. (1.12), provided the aperture is rectangular. We denote its length by a, its width by b; its area is A = ab. The integral equation (1.20) is now a two-dimensional version of Eq. (1.12). The mode subscripts become 2-vectors $\underset{\sim}{p} = (p_x, p_y)$ of integers p_x and p_y to account for the x- and y-directions.

The eigenvalues $h_{\underset{\sim}{p}}$ are now approximately

$$h_{\underset{\sim}{p}} \cong A_\delta \; B(p_x\delta_x, \; p_y\delta_y)/B_T, \tag{1.21}$$

where $\delta_x = \lambda R/a$, $\delta_y = \lambda R/b$, and $A_\delta = \delta_x\delta_y$. Here

$$B_T = \beta(0) = \int_O B(\underset{\sim}{u}) \; d^2\underset{\sim}{u} \tag{1.22}$$

is the integrated radiance of the object. The eigenfunction associated with $h_{\underset{\sim}{p}}$ is approximately

$$\eta_{\underset{\sim}{p}}'(\underset{\sim}{r}) \cong A^{-1/2} \exp[2\pi i(p_x x a^{-1} + p_y y b^{-1})]. \tag{1.23}$$

The eigenfunctions $\eta_{\underset{\sim}{p}}'(\underset{\sim}{r})$ depend only weakly on the actual distribution $B(\underset{\sim}{u})$ of the radiance, provided $B(\underset{\sim}{u})$ nowhere changes by very much over distances of the order of δ_x and δ_y.

When the area A_o of the object is so large that $A_o/\delta_x\delta_y \gg 1$, the eigenvalues $h_{\underset{\sim}{p}}$ are proportional to samples of the object radiance at points separated in x by $\delta_x = \lambda R/a$ and in y by $\delta_y = \lambda R/b$. The area $A_\delta = \delta_x\delta_y$ associated with each sampling point subtends from the aperture a solid angle of $A_\delta/R^2 = \lambda^2/A$. The number of significant spatial modes in the aperture field is roughly equal to $M = A_o/A_\delta = AA_o/\lambda^2R^2$. The highest spatial frequencies occurring in the significant modes are of the order of $a_o/\lambda R$ and $b_o/\lambda R$ in the x- and y-directions, where a_o and b_o are the length and breadth of the object. These spatial frequencies will be much less than $k/2\pi = \lambda^{-1}$ when $A_o << R^2$, that is, when the solid angle A_o/R^2 subtended by the object is much less than 1 steradian.

If a lens of focal length F is placed in the aperture, it focuses the object plane onto an image plane at a distance $R' = RF/(R + F)$ beyond the aperture. The component of the aperture field proportional to $\eta_p(\tilde{r})$ creates at point (x', y') in the image plane a field proportional to

$$\mathrm{sinc}[\pi(x' - \tilde{\xi}_{px})/\delta_x'] \; \mathrm{sinc}[\pi(y' - \tilde{\xi}_{py})/\delta_y'],$$
$$\delta_x' = \lambda R'/a, \quad \delta_y' = \lambda R'/b,$$

where

$$(\tilde{\xi}_{px}, \tilde{\xi}_{py}) = (p_x\delta_x', p_y\delta_y')$$

is the geometrical image of the object point $(p_x\delta_x, p_y\delta_y)$, and $\mathrm{sinc}\, x = (\sin x)/x$. Thus each spatial mode of the aperture field generates in the image plane the diffracted image of its associated object point. When $M = A_o/\delta_x\delta_y >> 1$, the mode expansion of the aperture field corresponds to the usual expansion of the field in the image plane through the Whittaker-Shannon sampling theorem.[15]

In this way the integral equations (1.13) and (1.20) permit a measure of the number of spatial degrees of freedom in the aperture field that contribute to detection and estimation of the object. The measure reduces to the generally accepted one at both extremes of complete first-order coherence ($A_o/\delta_x\delta_y << 1$) and extreme incoherence ($A_o/\delta_x\delta_y >> 1$), yet is definable through Eqs. (1.13) and (1.20) for intermediate degrees of first-order coherence as well.

Circular Aperture

For a circular aperture a general sampling approximation similar to Eq. (1.21) has not been discovered. If the radiance distribution of the object possesses circular symmetry, $B(\underset{\sim}{u}) = B(|\underset{\sim}{u}|)$, however, the eigenvalues are given approximately by

$$h_{kn} = (\lambda^2 R^2/AB_T)\ B(x_{km}\lambda R/2\pi a), \tag{1.24}$$

where a is the radius of the aperture and the numbers x_{kn} are the zeros of the Bessel function of order n,

$$J_n(x_{kn}) = 0, \quad k = 0, 1, 2, 3, \ldots \quad . \tag{1.25}$$

For n = 0 the eigenvalues have multiplicity 1, for m > 0 multiplicity 2. The derivation is presented in Appendix A.

When the object is a circle of area $A_o = \pi a_o^2$ radiating uniformly, the integral equation (1.20) reduces to the one treated by Slepian.[16] The mode functions $\eta_{kn}'(\underset{\sim}{r})$ are proportional to the generalized prolate spheroidal wave functions, and the associated eigenvalues are

$$h_{kn} = (4/\alpha^2)\ \lambda_{n,k}(\alpha),$$

$$\alpha = kaa_o/R = 2\pi aa_o/\lambda R, \tag{1.26}$$

where $\lambda_{n,k}$ are the eigenvalues tabulated by Slepian; our α corresponds to his parameter c. For $\alpha >> 1$ the number of significant eigenvalues is approximately

$$M = \alpha^2/4 = AA_o/\lambda^2 R^2, \tag{1.27}$$

those of multiplicity 2 being counted twice. The significance of the generalized prolate spheroidal wave functions for representing the field in the image plane has been pointed out by Toraldo di Francia.[5]

As Slepian has shown,[16] the eigenvalues $\lambda_{n,k}(\alpha)$ are small for $\alpha << 1$ and approach 1 exponentially when $\alpha >> 1$. According to Eq. (1.24), an eigenvalue $\lambda_{n,k}(\alpha)$ will be significantly large when the parameter α exceeds the corresponding zero x_{kn} of the Bessel function $J_n(x)$. For $\alpha = 10$, for instance, there are $2 \times 9 + 3 = 21$ zeros x_{kn} less than α, counting zeros with $n > 0$ twice. Of the corresponding eigenvalues $\lambda_{n,k}(10)$ the smallest is $\lambda_{6,0}(10) = 0.740$. For $\alpha = 10$, $M = \alpha^2/4 = 25$.

II. Quantum Detection

The Mode Operators

The decomposition of the aperture field into spatio-temporal modes can be used, as indicated by Kuriksha,[17] to derive the optimum detector of the light from an incoherently radiating object in the presence of thermal background light. The principal assumptions required are that the light from the object fall nearly perpendicularly upon the aperture from a cone of directions much narrower than 1 steradian and that the diameter of the aperture be much greater than the correlation length of the thermal light and the wavelength of the object light.

Quantum-mechanically the field at the aperture is treated as an operator. It is divided into its positive-frequency part $\psi_+(\underset{\sim}{r}, t)$ and its negative-frequency part $\psi_-(\underset{\sim}{r}, t)$, which are hermitian conjugate operators,

$$\psi_-(\underset{\sim}{r}, t) = [\psi_+(\underset{\sim}{r}, t)]^+. \tag{2.1}$$

Classically $\psi_+(\underset{\sim}{r}, t)$ corresponds to the analytic signal. The mutual coherence function of the aperture field is

$$\varphi(\underset{\sim}{r}_1, t_1; \underset{\sim}{r}_2, t_2) = \mathrm{Tr}[\rho\psi_-(\underset{\sim}{r}_2, t_2)\ \psi_+(\underset{\sim}{r}_1, t_1)], \tag{2.2}$$

where Tr stands for the trace and ρ is the density operator of the field.[8] When the object is present, φ is the sum of φ_s and φ_n as given by Eqs. (1.2) and (1.3); when the object is absent, $\varphi = \varphi_n$.

The field operator $\psi_+(r, t)$ is expanded in the spatio-temporal modes defined by Eqs. (1.10) and (1.11). The coefficients of this expansion are proportional to the quantum-mechanical operators

$$b_{\underset{\sim}{p}m} = (2\Omega c/\hbar)^{1/2} \int_A \int_0^T e^{i\Omega t}\ \eta_{\underset{\sim}{p}}^*(\underset{\sim}{r})\ \gamma_m^*(t)\ \psi_+(\underset{\sim}{r}, t)\ d^2\underset{\sim}{r}dt. \tag{2.3}$$

In the expansion of $\psi_-(\underset{\sim}{r}, t)$ the hermitian conjugate operators

$$b_{\underset{\sim}{qn}}{}^{+} = (2\Omega c/\hbar)^{1/2} \int_A \int_0^T e^{-i\Omega t} \, \eta_{\underset{\sim}{q}}(\underset{\sim}{r}) \, \gamma_n(t) \, \psi_-(\underset{\sim}{r}, t) \, d^2\underset{\sim}{r} dt \tag{2.4}$$

appear. Under the assumptions stated at the beginning, these operators commute for different spatio-temporal modes; specifically, their commutators are

$$\begin{aligned} &[b_{\underset{\sim}{pm}}, b_{\underset{\sim}{qn}}{}^{+}] = b_{\underset{\sim}{pm}} b_{\underset{\sim}{qn}}{}^{+} - b_{\underset{\sim}{qn}}{}^{+} b_{\underset{\sim}{pm}} = \delta_{\underset{\sim}{pq}} \delta_{mn}, \\ &[b_{\underset{\sim}{pm}}, b_{\underset{\sim}{qn}}] = [b_{\underset{\sim}{pm}}{}^{+}, b_{\underset{\sim}{qn}}{}^{+}] = 0. \end{aligned} \tag{2.5}$$

These operators play the same role as the ordinary creation and annihilation operators for the spatial modes of the electromagnetic field when quantized in a closed volume.[6,18]

To derive the first of these commutation relations, the commutator of the operators $\psi_+(\underset{\sim}{r}_1, t_1)$ and $\psi_-(\underset{\sim}{r}_2, t_2)$ is used; it is proportional to the positive-frequency part of Green's function for the free scalar field,[18]

$$\begin{aligned} &[\psi_+(\underset{\sim}{r}_1, t_1), \psi_-(\underset{\sim}{r}_2, t_2)] = \\ &\tfrac{1}{2}\hbar(2\pi)^{-3} \iiint \omega^{-1} \exp[-i\omega(t_1 - t_2) + i\underset{\sim}{k}\cdot(\underset{\sim}{r}_1 - \underset{\sim}{r}_2)] \, d^3\underset{\sim}{k}, \\ &\omega^2 = c^2\underset{\sim}{k}^2 = c^2(k_x{}^2 + k_y{}^2 + k_z{}^2). \end{aligned} \tag{2.6}$$

Using Eqs. (2.3), (2.4), and (2.6), we find

$$\begin{aligned} [b_{\underset{\sim}{pm}}, b_{\underset{\sim}{qn}}{}^{+}] = (\Omega/8\pi^3 c) &\int_A \int_0^T \int_A \int_0^T \iiint |k_z|^{-1} \, \eta_{\underset{\sim}{p}}{}^*(\underset{\sim}{r}_1) \, \gamma_m{}^*(t_1) \\ &\times \eta_{\underset{\sim}{q}}(\underset{\sim}{r}_2) \, \gamma_n(t_2) \exp[i(\Omega - \omega)(t_1 - t_2) + i\underset{\sim}{k}\cdot(\underset{\sim}{r}_1 - \underset{\sim}{r}_2)] \\ &\times d^2\underset{\sim}{r}_1 d^2\underset{\sim}{r}_2 dt_1 dt_2 dk_x dk_y d\omega. \end{aligned} \tag{2.7}$$

In the process we have changed integration variables from (k_x, k_y, k_z) to (k_x, k_y, ω), with $\omega d\omega = c^2|k_z|dk_z$. In Eq. (2.7),

$$\underset{\sim}{k} \cdot (\underset{\sim}{r}_1 - \underset{\sim}{r}_2) = k_x(x_1 - x_2) + k_y(y_1 - y_2),$$

z_1 and z_2 having been set equal to 0 for points on the aperture.

The right-hand side of Eq. (2.7) contains the Fourier transforms of $\gamma_m^*(t_1)$ and $\gamma_n(t_2)$. We have seen in Section I that the largest frequencies in these functions are of the order of W. Hence in the integration over ω in Eq. (2.7) a significant contribution will be made only by values of ω within about W of Ω, and $W << \Omega$. The multiple integral also contains the spatial Fourier transforms of $\eta_{\underset{\sim}{p}}^*(\underset{\sim}{r}_1)$ and $\eta_{\underset{\sim}{q}}(\underset{\sim}{r}_2)$. The highest spatial frequencies in these functions are much less than $k = 2\pi/\lambda$ when, as assumed, the object subtends a solid angle much less than 1 steradian. Hence, to the integration over k_x and k_y in Eq. (2.7) only values of k_x and k_y much less than $k = \omega/c$ contribute. It is therefore an accurate approximation to set

$$|k_z| = (\omega^2 c^{-2} - k_x^2 - k_y^2)$$

equal to Ω/c and take it outside the integral. The integrations over ω, k_x, and k_y now lead to delta-functions, and when these are integrated out and the orthonormality of the mode functions is used, the first part of Eq. (2.5) results. The second part follows immediately from the commutator

$$[\psi_+(\underset{\sim}{r}_1, t_1), \psi_+(\underset{\sim}{r}_2, t_2)] = 0$$

and its hermitian conjugate.

The mode operators $b_{\underset{\sim}{p}m}$, $b_{\underset{\sim}{q}n}^+$ are not ordinary quantum-mechanical operators because they possess no time dependence. They are determined, as in Eqs. (2.3) and (2.4), by integrals of the aperture field over two spatial dimensions and over time. Despite this unusual character, the operators for different modes are in principle measurable simultaneously. In back of the aperture a large, lossless cavity is placed, as described in III. Initially empty, it is exposed to the aperture field during the interval (0, T), after which it is closed.

The operators $\tilde{b}_{pm}$ and $\tilde{b}_{qn}^{+}$ can be expressed as linear combinations of the creation and annihilation operators of the cavity modes at any later time $t > T$ by applying the technique developed in III. Since $\tilde{b}_{pm}$ and $\tilde{b}_{qn}^{+}$ commute, so do those linear combinations and are hence measurable by suitable observations of the cavity field.

The Optimum Detector

Both the object and the background contain a great many atoms, ions, and electrons radiating independently. The density matrices ρ_0 and ρ_1 describing the field under the two hypotheses H_0 (object absent) and H_1 (object present) have, therefore, gaussian P-representations.[19] These depend only on the mode correlation matrices $\mathrm{Tr}(\rho_i b_{\tilde{q}n}^{+} b_{\tilde{p}m})$, $i = 0, 1$, which are related through Eqs. (2.3) and (2.4) to the mutual coherence functions of the aperture field under H_0 and H_1.

Because the diameter of the aperture is much greater than the correlation length of the background field, and because the rays from the object are paraxial, the mutual coherence function φ_n of the background light can be expressed in the delta-function form of Eq. (1.2), as discussed in III, Section IV. Furthermore, the mode functions are eigenfunctions of the mutual coherence function of the object light, Eq. (1.9). As a consequence of Eqs. (1.2) and (1.9) and of the orthonormality of the mode functions--Eq. (1.8)--, the mode correlation matrices $\mathrm{Tr}(\rho_i b_{\tilde{q}n}^{+} b_{\tilde{p}m})$ under both hypotheses are diagonal. The modes are statistically independent and can be treated separately. Furthermore, the density matrices ρ_0 and ρ_1 now depend only on the number operators $n_{\tilde{p}m} = b_{\tilde{p}m}^{+} b_{\tilde{p}m}$ of the modes, and because of Eq. (2.5) these commute and are simultaneously measurable.

The operator $n_{\tilde{p}m}$ determines the excitation level or number of photons in the spatio-temporal mode $(\tilde{p}m)$. The outcome $n'_{\tilde{p}m}$ of a measurement of $n_{\tilde{p}m}$ is an integral-valued random variable with an exponential distribution,[19,20]

$$p_i(n'_{\tilde{p}m}) = (1 - v_{\tilde{p}m}^{(i)}) \exp(n'_{\tilde{p}m} \ln v_{\tilde{p}m}^{(i)}),$$

$$v_{\tilde{p}m}^{(i)} = N_{\tilde{p}m}^{(i)}/(N_{\tilde{p}m}^{(i)} + 1), \quad i = 0, 1, \tag{2.8}$$

where

$$N_{\underset{\sim}{pm}}^{(0)} = \mathfrak{N} = [\exp(\hbar\Omega/K\mathcal{T}) - 1]^{-1} \tag{2.9}$$

and

$$N_{\underset{\sim}{pm}}^{(1)} = \mathfrak{N} + h_{\underset{\sim}{p}} g_m N_s . \tag{2.10}$$

Here K is Boltzmann's constant, $\mathcal{T}$ is the effective absolute temperature of the background light, and $N_s = E_s/\hbar\Omega$ is the average total number of photons received at the aperture A from the object during (0, T). It has been assumed in Eq. (2.9) that all significant modes have the same frequency Ω; the differences are at most of the order of $W \ll \Omega$.

The independence of the modes permits basing the optimum detector on the logarithmic likelihood ratio[4]

$$U = \ln \prod_{\underset{\sim}{p},m} p_1(n'_{\underset{\sim}{pm}})/p_0(n'_{\underset{\sim}{pm}}) =$$

$$\sum_{\underset{\sim}{p},m} \{n'_{\underset{\sim}{pm}} \ln(v_{\underset{\sim}{pm}}^{(1)}/v_{\underset{\sim}{pm}}^{(0)}) + \ln[(1 - v_{\underset{\sim}{pm}}^{(1)})/(1 - v_{\underset{\sim}{pm}}^{(0)})]\}. \tag{2.11}$$

The detector chooses H_1, deciding that the object is present, if U exceeds a decision level U_0, which can be set to provide a pre-assigned false-alarm probability

$$Q_0 = \Pr(U > U_0|H_0).$$

In the quantum limit $N_{\underset{\sim}{pm}}^{(1)} \ll 1$, $\mathfrak{N} \ll 1$, and $v_{\underset{\sim}{pm}}^{(i)} \doteq N_{\underset{\sim}{pm}}^{(i)}$, whereupon the logarithmic likelihood ratio is approximately

$$U = \sum_{\underset{\sim}{p},m} [n'_{\underset{\sim}{pm}} \ln(1 + h_{\underset{\sim}{p}} g_m N_s/\mathfrak{N}) - h_{\underset{\sim}{p}} g_m N_s]. \tag{2.12}$$

If, as we are generally assuming, the spectral density of the object light is uniform over a frequency interval of width W about $\Omega/2\pi$, and $WT \gg 1$, the eigenvalues g_m can be set equal to $(WT)^{-1}$, and the statistic U can be written as a sum over only spatial modes,

$$U = \sum_{\underset{\sim}{p}} [n_{\underset{\sim}{p}} \ln(1 + h_{\underset{\sim}{p}} N_s/\mathfrak{N}WT) - h_{\underset{\sim}{p}} N_s], \tag{2.13}$$

where

$$n_{\mathbf{p}} = \sum n'_{\mathbf{p}m} \tag{2.14}$$

is the total number of photons counted in spatial mode $\mathbf{p}$ during $(0, T)$. The optimum detector weights these numbers logarithmically in accordance with the expected number $N_{\mathbf{p}s} = h_{\mathbf{p}} N_s$ of photons received in that mode from the object when present.

When the object is a point source, only a single spatial mode is significant, and the decision can be based on the total number n_1 of photons counted at the aperture. Since $WT \gg 1$, that number has a Poisson distribution under both hypotheses H_0 and H_1. The probability $Q_d = \Pr\{U > U_0 | H_1\}$ of detecting the object can be calculated as described in III, Section V, where Q_d is plotted as a function of the average number N_s of signal photons for various values of $N_0 = \mathcal{N}WT$.

When the object is extensive, $A_o/\delta_x\delta_y \gg 1$, yet $A_o \ll R^2$, focusing the object plane onto an image plane associates each significant spatial mode $\eta_{\mathbf{p}}(\mathbf{r})$ in the aperture with a diffraction pattern in the image plane. The pattern is centered at the geometrical image of the associated object point $(p_x \delta_x, p_y \delta_y)$. Suppose the image plane to contain a mosaic of photosensitive spots just coinciding with the central peaks of each of these diffraction patterns. If their quantum efficiency equaled 1, the number of photoelectrons each spot emitted would be nearly equal to the number $n_{\mathbf{p}}$ for the associated spatial mode, and a detector that weighted those numbers of photoelectrons as in Eq. (2.13) would be nearly equivalent to the optimum detector. Such a detector has been analyzed previously.[21]

The Threshold Detector

The optimum detector specified by Eq. (2.13) and depending through N_s on the total radiant power B_T of the object does not provide a uniformly most powerful test.[22] It must be set up for a standard object of radiance proportional to $B(\underset{\sim}{u})$ and total power $B_T^{(0)}$, and it will provide suboptimum detection of objects of different total power B_T.

A detector that is independent of knowledge of B_T, yet nearly as good as the optimum, is obtained by replacing the logarithm in Eq. (2.12) by the first term of its Taylor expansion. The constant factor $N_s/\mathfrak{N}$ can be cancelled from both statistic and decision level, and the new detector is equivalent to one basing its decision on the operator

$$U' = \sum_{\underset{\sim}{p},m} h_{\underset{\sim}{p}} g_m n_{\underset{\sim}{p}m} = \sum_{\underset{\sim}{p},m} h_{\underset{\sim}{p}} g_m b_{\underset{\sim}{p}m}^{+} b_{\underset{\sim}{p}m} . \tag{2.15}$$

This is the threshold detector derived in III. By using the definitions in Eqs. (2.3) and (2.4) and the orthonormality of the mode functions, U' can be written as a bilinear integral form in the field operators $\psi_-(\underset{\sim}{r}, t)$ and $\psi_+(\underset{\sim}{r}, t)$, with a result differing only by an inconsequential constant factor from III, Eq. (4.18). When $g_m \equiv (WT)^{-1}$, the threshold detector bases its decisions on the weighted sum

$$U'' = \sum_{\underset{\sim}{p}} h_{\underset{\sim}{p}} n_{\underset{\sim}{p}} \tag{2.16}$$

of the numbers $n_{\underset{\sim}{p}}$ of photons counted in the spatial modes $\underset{\sim}{p}$ during the interval (0, T).

When M = 1, the threshold and optimum detectors are identical, basing their decisions on the total number n_1 of photons observed at the aperture. When M >> 1, as we have seen, there are about M spatial modes with nearly equal eigenvalues $h_{\underset{\sim}{p}} \cong M^{-1}$, and both the threshold and the optimum detectors sum the numbers $n_{\underset{\sim}{p}}$ of photons in these modes with approximately a uniform weighting. The two detectors differ only in their treatment of modes whose eigenvalues are rather less than M^{-1}, and these contribute relatively little to the statistics U or U". Hence, when their decision levels are adjusted to provide equal false-alarm probabilities Q_0, the threshold and the optimum detectors attain nearly the same probability of detection.

Detectability of a Circular Object

When the object radiates uniformly over a circle of radius a_0 and the aperture is a circle of radius a, the eigenvalues $h_{\underset{\sim}{p}} = h_{kn}$ determining the detection statistic and the probability of detection are given by Eq. (1.26) in terms of the eigenvalues tabulated by Slepian.[16] To illustrate the dependence of the probability of detection on the degree of coherence of the object light reaching the aperture, we have calculated it for the threshold detector,

$$Q_d = \Pr\{U'' > U_0 | H_1\},$$

as a function of the average total number N_s of photons from the object. The decision level U_0 was set to attain a false-alarm probability

$$Q_0 = \Pr\{U'' > U_0 | H_0\}$$

equal to 0.01, and the value of $N_0 = \mathfrak{N}WT$ was set equal to 1.0. The results are plotted in Fig. 1 for various values of $\alpha = 2\pi a a_0/R\lambda$.

For $\alpha = 0$ a single spatial mode contributes to the detection, and the optimum and threshold detectors are the same. The number of photons observed has a Poisson distribution, and the detection probability is calculated by III, Eqs. (5.17) - (5.19). For $\alpha = 1$ four terms and for $\alpha = 2$ five terms in the sum in Eq. (2.16) were used, corresponding to the four or five largest eigenvalues h_{kn}, and a computer was programmed to add up the joint Poisson probabilities of all sets of numbers $n_{\underset{\sim}{p}}$ for which the sum U'' is less than U_0; Q_d is equal to 1 minus this total probability. Taking seven terms for $\alpha = 2$ changed the detection probabilities only slightly, but greatly increased computation time.

For $\alpha \geqslant 4$ the moment-generating function (m. g. f.) of the statistic U'',

$$\mu(s; N_s) = \underset{\sim}{E}\,[\exp(sU'') | H_1] =$$
$$\exp\Big[\sum_{k,n} (N_0 + N_s h_{kn}) \exp(h_{kn} s)\Big], \tag{2.17}$$

was used to calculate the detection probability. The false-alarm probability Q_0 is the inverse Laplace transform of $[1 - \mu(-s; 0)]/s$ evaluated at $U'' = U_0$, and this was approximated by the method of steepest descent, as in III, Eq. (5.23). By means of Newton's method the decision level U_0 yielding $Q_0 = 0.01$ was determined. The detection probabilities were then computed by summing the Gram-Charlier series,[23] whose coefficients are calculated by expanding $\ln \mu(s; N_s)$ in a power series at $s = 0$. Terms in the series were summed as long as they decreased, and the summation was stopped when the terms began to increase again, consistently with the asymptotic nature of the Gram-Charlier series.

In order to compare the threshold detector with the optimum, the detection probabilities attained by the latter were also calculated for $\alpha = 4$, 6, and 8. The optimum detector was set up for a standard number $N_s^{(0)}$ of signal photons equal to 8; $N_0 = \mathfrak{N}WT = 1$. The moment-generating function for the optimum statistic U is the same as in Eq. (2.17), except that $\exp(h_{km}s)$ is replaced by $\exp[s \ln (1 + N_s^{(0)} h_{km}/N_0)]$, and the same method of computation was used. The differences between the detection probabilities for the optimum and threshold detectors were of the order of the inaccuracy in the numerical calculations and too small to show up on the graph in Fig. 1.

The results demonstrate the slight difference between the performances of the optimum and the threshold detectors, and they show how, for a fixed false-alarm probability Q_0, the detection probability decreases as the object light is divided among more and more spatially incoherent degrees of freedom.

Detectability of Large Objects

The logarithm of the moment-generating function of the threshold operator U' in Eq. (2.15) is

$$\ell n\ \mu(s) = \underset{\sim}{E}(e^{sU'}\ |H_1) =$$

$$-\sum_{\underset{\sim}{p},m} \ell n\{1 - N^{(1)}_{\underset{\sim}{p}m}\ [\exp(h_{\underset{\sim}{p}}g_m s) - 1]\} \tag{2.18}$$

with the mean value $N^{(1)}_{\underset{\sim}{p}m}$ given by Eq. (2.10). Since $N^{(1)}_{\underset{\sim}{p}m} << 1$ under quantum-limited conditions, this is approximately

$$\ell n\ \mu(s) = \sum_{\underset{\sim}{p},m} (\mathfrak{N} + h_{\underset{\sim}{p}}g_m N_s)\ [\exp(h_{\underset{\sim}{p}}g_m s) - 1]. \tag{2.19}$$

When the object contains many degrees of freedom, $MWT >> 1$, the sum over the spatio-temporal modes can be replaced by an integration over temporal frequency and over the object by substituting from Eqs. (1.15) and (1.21). The result is

$$\ell n\ \mu(s) = \mathfrak{N} MT \int_O \int (d^2\underset{\sim}{u}/A_o) \int_{-\infty}^{\infty} (d\omega/2\pi)$$

$$\times\ [1 + N_s\ B(\underset{\sim}{u})\ X(\omega)/\bar{B}\mathfrak{N} MT]$$

$$\times\ \{\exp[B(\underset{\sim}{u})\ X(\omega)s/\bar{B}MT] - 1\}, \tag{2.20}$$

where $\bar{B} = B_T/A_o$ is the average radiance of the object and $M = AA_o/\lambda^2R^2$ is its effective number of degrees of freedom. This corresponds to III, Eq. (5.14) for a point object of arbitrary spectral density $X(\omega)$. An expansion of $\ell n\ \mu(s)$ in powers of s yields the cumulants of the distribution of the statistic U', from which the coefficients of the Gram-Charlier series can be calculated.[23] An example of a point object with a Lorentz spectrum was described in III, Section V.

III. Estimation of Object Radiance

We have seen in Section I that the eigenvalues $h_{\tilde{p}}$ of the spatial modes are proportional to samples of the radiance distribution $B(\tilde{u})$ of the object when the aperture is rectangular and the object so large that $M = AA_0/\lambda^2R^2 >> 1$. The mode functions are in this approximation independent of the actual form of $B(\tilde{u})$. The aperture field can therefore be expanded in spatial modes without knowledge of the true distribution of radiance in the object plane, and the strength of each mode in the component of the aperture field due to the object is proportional to the radiance $B(\tilde{u})$ at a particular point of the object.

The random coefficients of this expansion in spatial modes will be statistically independent. It is possible, therefore, to estimate the radiance $B(\tilde{u})$ at points on the object spaced by $\delta_x = \lambda R/a$ in the x-direction and by $\delta_y = \lambda R/b$ in the y-direction, and these estimates can be made independently. Conversely, it is to be expected that $B(\tilde{u})$ cannot be estimated at a finer grid of sample points by any method that does not require simultaneous calculations involving all the points.

A lower bound to the relative mean-square error of an unbiased estimate of the radiance $B_{\tilde{p}} = B(\tilde{u}_{\tilde{p}})$ at the sample point $\tilde{u}_{\tilde{p}} = (p_x \delta_x, p_y \delta_y)$ can be calculated by means of the Cramér-Rao inequality.[24-26] As might be expected, this lower bound is the same as that determined in IV for the relative mean-square error of the radiant power of a point source.

Since the number operators $n_{\tilde{p}m} = b_{\tilde{p}m}^{+} b_{\tilde{p}m}$ for the spatio-temporal modes commute and can be measured simultaneously, the classical-statistical form of the Cramér-Rao inequality can be used, and since the modes are statistically independent, they can be treated separately. The data for estimating $B_{\tilde{p}}$ are the observed numbers $n'_{\tilde{p}m}$ of photons in the modes $(\tilde{p}m)$, whose joint probability is, as in Eq. (2.8),

$$p(\{n'_{pm}\};\ \theta) = \prod_m (1 - v_{pm}) \exp(n'_{pm} \ln v_{pm}),$$

$$v_{pm} = N_{pm}/(1 + N_{pm}), \tag{3.1}$$

where

$$N_{pm} = \mathfrak{N} + g_m\theta \tag{3.2}$$

with $\theta = h_p N_s$ proportional to B_p through an equation like Eq.(1.21).

The mean-square error of an unbiased estimate $\hat{\theta}$ of θ is bounded below by

$$E(\hat{\theta} - \theta)^2 > \{E[\frac{\partial}{\partial\theta} \ln p(\{n'_{pm}\};\ \theta)]^2\}^{-1}$$

$$= \{\sum_m [g_m{}^2/N_{pm}(1 + N_{pm})]\}^{-1}. \tag{3.3}$$

By use of Eq. (1.15) and the inequalities

$$WT >> 1, \qquad N_{pm} << 1,$$

the sum over m can be approximated by an integral over frequency involving the spectral density $X(\omega)$ of the object light. As a result the relative mean-square error in an unbiased estimate of θ or B_p is bounded below by

$$E(\hat{B}_p - B_p)^2/B_p{}^2 \geq N_{ps}{}^{-1}[f_1(\mathscr{D}_p)]^{-1},$$

$$\mathscr{D}_p = N_{ps}/\mathfrak{N}WT, \tag{3.4}$$

where $N_{ps} = h_p N_s$ is the total average number of photons received from the object in spectral mode p, that is, from an area $A_\delta = \delta_x\delta_y$ of the object about u_p. The function $f_1(\mathscr{D})$ is the same as in IV, Eq. (3.4),

$$f_1(\mathscr{D}) = \mathscr{D}W\int_{-\infty}^{\infty} [X(\omega)]^2[1 + \mathscr{D}WX(\omega)]^{-1}\ d\omega/2\pi, \tag{3.5}$$

and Eq. (3.4) corresponds to IV, Eq. (4.6) for the relative mean-square error in the radiant power of a point object.

When the spectral density of the object is rectangular, the total number

$$n_{\tilde{p}} = \sum_m n'_{\tilde{p}m}$$

of photons from all temporal modes in spatial mode $\tilde{p}$ is a sufficient estimator of the parameter θ or, equivalently, of the radiance $B_{\tilde{p}}$ at the sample point $\tilde{u}_{\tilde{p}}$ on the object.[24,26] It provides an unbiased estimate after the known average contribution $N_0 = \mathfrak{N} WT$ of the background is subtracted, and the relative mean-square error of the estimate is given by the right-hand side of Eq. (3.4), where now

$$f_1(\mathscr{D}) = \mathscr{D}/(\mathscr{D} + 1).$$

Under extreme quantum-limited conditions the minimum relative mean-square error in an estimate $\hat{B}_{\tilde{p}}$ is equal to $N_{\tilde{p}s}^{-1}$, where $N_{\tilde{p}s}$ is the average number of photons received during $(0, T)$ from the element of area $\delta_x \delta_y$ about the point $(p_x \delta_x, p_y \delta_y)$. Under a background limitation $(K\mathcal{T} \gg \hbar\Omega)$, the minimum mean-square error is, as in I, Eq. (6.3),

$$\tilde{E}(\hat{B}_{\tilde{p}} - B_{\tilde{p}})^2/B_{\tilde{p}}^2 = (N'/E_{\tilde{p}s})^2 \, WT,$$

where $E_{\tilde{p}s} = N_{\tilde{p}s}\hbar\Omega$ is the total average energy received from the area $\delta_x\delta_y$ about $\tilde{u}_{\tilde{p}}$, and $N' = K\mathcal{T}$ is the spectral density of the background light, assumed spatially and temporally white.

Appendix

Approximate Eigenvalues of a Circularly Symmetrical Kernel

Dropping the primes on the eigenfunctions in Eq. (1.20) and writing $\psi(\underset{\sim}{r})$ for $\beta(\underset{\sim}{r})/A\beta(0)$, we study the integral equation

$$h_{km}\,\eta_{km}(\underset{\sim}{r}) = \int_A \psi(\underset{\sim}{r} - \underset{\sim}{s})\;\eta_{km}(\underset{\sim}{s})\;d^2\underset{\sim}{s}, \tag{A1}$$

in which $\psi(\underset{\sim}{r})$ is assumed to be a function of $r = |\underset{\sim}{r}|$ only. Its Fourier transform

$$\Psi(\underset{\sim}{\rho}) = \Psi(\rho) = \int \psi(\underset{\sim}{r})\;\exp(-i\underset{\sim}{\rho}\cdot\underset{\sim}{r})\;d^2\underset{\sim}{r} \tag{A2}$$

is a function only of $\rho = |\underset{\sim}{\rho}|$. (Unmarked integrals are taken over all of two-dimensional space.) Therefore,[27]

$$\psi(\underset{\sim}{r} - \underset{\sim}{s}) = \int \Psi(\underset{\sim}{\rho})\;\exp[i\underset{\sim}{\rho}\cdot(\underset{\sim}{r} - \underset{\sim}{s})]\;d^2\underset{\sim}{\rho}/(2\pi)^2$$

$$= \int_0^\infty \rho\Psi(\rho)\;J_0(\rho|\underset{\sim}{r} - \underset{\sim}{s}|)\;d\rho/2\pi =$$

$$\sum_{m=0}^{\infty} (2 - \delta_{m0}) \int_0^\infty \rho\Psi(\rho)\;J_m(\rho r)\;J_m(\rho s)\;\cos m(\theta_r - \theta_s)\;d\rho, \tag{A3}$$

where $s = |\underset{\sim}{s}|$ and θ_r and θ_s are the polar angles of the points $\underset{\sim}{r}$ and $\underset{\sim}{s}$, respectively.

We assume to start with that the eigenfunction $\eta_{km}(\underset{\sim}{s})$ is given for $m > 0$ by

$$\eta_{km}(\underset{\sim}{s}) = C_{km}\;J_m\;(b_{km}s)\;\cos m\theta_s, \tag{A4}$$

where C_{km} is a normalizing constant and $x_{km} = b_{km}a$ is the k-th zero of the Bessel function $J_m(x)$; $\underline{a}$ is the radius of the aperture. It will appear later that this assumption is approximately correct when the radius $\underline{a}$ of the aperture is much greater than the width of $\psi(\underset{\sim}{r})$. A second set of eigenfunctions is, for $m > 0$,

$$\eta_{km}(\underset{\sim}{s}) = C_{km}\, J_m(b_{km}s)\, \sin m\theta_s ; \tag{A5}$$

the derivation to follow goes through for them as well, and the resulting eigenvalues h_{km} are the same. For $m = 0$ the eigenfunctions are, still approximately,

$$\eta_{k0}(\underset{\sim}{s}) = C_{k0}\, J_0(b_{k0}s). \tag{A6}$$

Thus the eigenvalues h_{km} have multiplicity 1 for $m = 0$ and multiplicity 2 for $m > 0$. All these eigenfunctions are orthogonal over the circle $0 \le s \le a$, $0 \le \theta_s < 2\pi$.

Substituting from Eqs. (A3) and (A4) into Eq. (A1) and integrating over θ_s, we find

$$h_{km}\, \eta_{km}(\underset{\sim}{r}) = C_{km} \cos m\theta_r \times \int_0^\infty \rho d\rho \int_0^a sds\, \Psi(\rho)\, J_m(\rho r)\, J_m(\rho s)\, J_m(b_{km}s)$$

$$= C_{km} \cos m\theta_r \int_0^\infty \rho\Psi(\rho)\, F_{km}(\rho)\, J_m(\rho r)\, d\rho, \tag{A7}$$

where[27]

$$F_{km}(\rho) = \int_0^a s\, J_m(\rho s)\, J_m(b_{km}s)\, ds$$

$$= (\rho^2 - b_{km}{}^2)^{-1}\, b_{km}a\, J_m{}'(b_{km}a)\, J_m(\rho a). \tag{A8}$$

The function $F_{km}(\rho)$ is sharply peaked near $\rho = b_{km}$; its width is of the order of a^{-1}. When the width of $\psi(\underset{\sim}{r})$ is much less than a, its Fourier transform $\Psi(\rho)$ is nearly constant for changes in ρ of the order of a^{-1}. Therefore, we can put $\Psi(\rho) = \Psi(b_{km})$ in the integrand of Eq. (A7) and take it outside the integral. The integration over ρ in the first part of the right-hand side of Eq. (A7) can now be carried out; it represents the closure relation for the Fourier-Bessel transform and yields a delta function $s^{-1}\delta(r - s)$. Upon integrating over s, we get approximately

$$h_{km}\,\eta_{km}(\underset{\sim}{r}) = C_{km}\,\Psi(b_{km})\,J_m(b_{km}r)\cos m\theta_r, \tag{A9}$$

verifying our choice in Eq. (A4) of the approximate eigenfunctions. Hence $h_{km} = \Psi(b_{km})$, and translating this result into the notation of Section I, we obtain Eq. (1.24).

Acknowledgment

I wish to thank Mr. Yie-Ming Hong for programming the calculations of detection probabilities by the digital computer. I am grateful to Dr. David Slepian of the Bell Telephone Laboratories, Inc., for supplying a program to calculate the generalized prolate spheroidal wavefunctions and their eigenvalues.

Footnotes

* This research has been carried out under NASA Grant No. 05-009-079.

1. C. W. Helstrom, J. Opt. Soc. Am. 59, 164 (1969), herein referred to as I.

2. C. W. Helstrom, J. Opt. Soc. Am. 59, 331 (1969) (II).

3. D. Middleton, An Introduction to Statistical Communication Theory, (McGraw-Hill Book Co., New York, 1960), Chs. 18-22.

4. C. W. Helstrom, Statistical Theory of Signal Detection, (Pergamon Press, Ltd., Oxford, 1968), 2nd. Ed., Chs. 3, 8.

5. G. Toraldo di Francia, J. Opt. Soc. Am. 59, 799 (1969). This paper provides references to previous work on image degrees of freedom.

6. W. Louisell, Radiation and Noise in Quantum Electronics (McGraw-Hill Book Co., New York, 1964), Ch. 4.

7. Ref. 4, pp. 69-72; ref. 1, Section I.

8. C. W. Helstrom, J. Opt. Soc. Am. 59, (1969), herein referred to as III.

9. Ref. 4, Ch. 11, §1 (iii), p. 383.

10. Ref. 8, Section V and Appendix.

11. U. Grenander and G. Szegö, Toeplitz Forms and Their Applications (Univ. of California Press, Berkeley, 1958), §8.6, pp. 136-139.

12. D. Slepian and H. O. Pollak, Bell Sys. Tech. J. 40, 43 (1961).

13. See ref. 1, Eqs. (1.8), (1.9), (A2).

14. C. W. Helstrom, "Estimation of Object Parameters by a Quantum-Limited Optical System", submitted to J. Opt. Soc. Am, and herein referred to as IV. See Section IV.

15. D. Gabor, "Light and Information", Progress in Optics (E. Wolf, ed., North-Holland Publishing Co., Amsterdam), 1, 109 (1961). See p. 138.

16. D. Slepian, Bell Sys. Tech. J. 43, 3009 (1964).

17. A. Kuriksha, Radio Engrg. and Electronic Phys. 13, 1567 (1968).

18. G. Wentzel, Quantum Theory of Fields (Interscience Publishers, New York and London, 1949), Ch. I.

19. R. J. Glauber, Phys. Rev. 131, 2766 (1963), Section VIII.

20. Ref. 6, §6.10, pp. 242-245.

21. C. W. Helstrom, Trans. IEEE, IT-10, 275 (1964).

22. Ref. 4, p. 152.

23. Ref. 4, p. 219.

24. H. Cramér, Mathematical Methods of Statistics (Princeton University Press, 1946), pp. 473 ff.

25. See also I, Section VI, and IV.

26. Ref. 4, pp. 260-261.

27. Here we have used Eq. 7.3.1(2), p. 14, and Eq. 7.15(31), p. 101 in A. Erdélyi et al. (eds.), Higher Transcendental Functions (McGraw-Hill Book Co., New York, 1953), vol. 2.

28. Ref. 26, Eq. 7.14.1(9), p. 90.

Figure Caption

Fig. 1. Probability Q_d of detecting a uniform circular object of radius a_o by observations at an aperture of radius a, versus the average number N_s of photons received from the object. The average number of background photons is $N_0 = \mathfrak{N}WT = 1.0$; the false alarm probability is $Q_0 = 0.01$. The curves are indexed by the parameter $\alpha = 2\pi a a_o/\lambda R$.

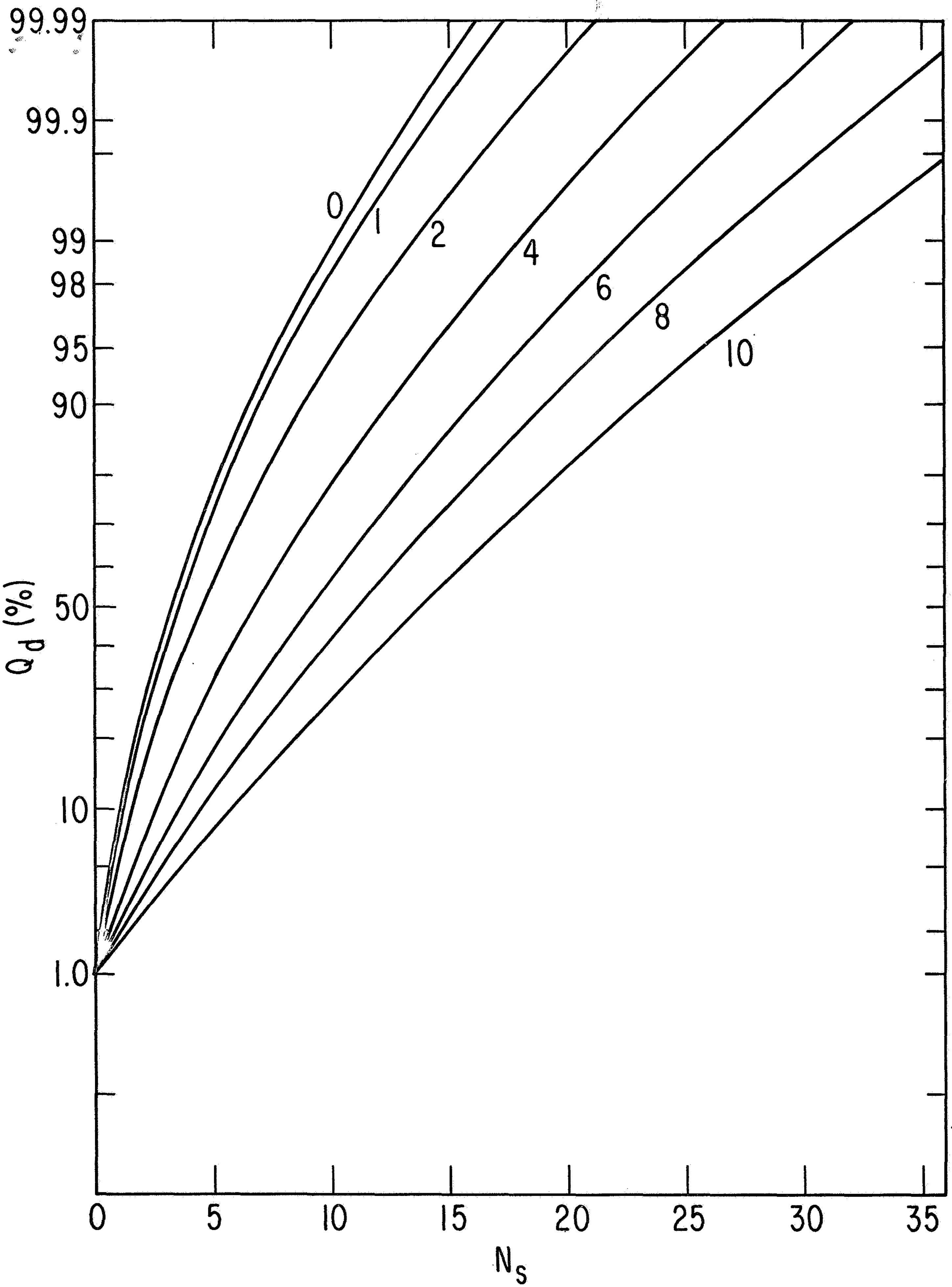

99.99
99.9
99
98
95
90
50
10
1.0
Q_d (%)
0
1
2
4
6
8
10
0
5
10
15
20
25
30
35
N_s

Some Integrals Involving Legendre Polynomials*

The following integrals have not been found in any of the readily available formularies. In (1) through (4) $P_n(x)$ is the Legendre polynomial of order n, and m and n are both odd.

$$\int_{-1}^{1} x^{-2}[P_n(x)]^2\, dx = 2, \tag{1}$$

$$\int_{-1}^{1} x^{-2}\, P_m(x)\, P_n(x)\, dx = 2(-1)^{(m-n)/2} \frac{(m-1)(m-3)\ldots(n+1)}{m\quad(m-2)\ldots(n+2)},$$

$$m > n, \tag{2}$$

$$\int_{-1}^{1} x^{-1}P_{n+1}(x)\, P_m(x) = 0, \quad m \le n, \tag{3}$$

$$\int_{-1}^{1} x^{-1}P_{n+1}(x)\, P_m(x) = 2(-1)^{(m-n-2)/2} \frac{(m-1)(m-3)\ldots(n+3)}{m(m-2)\ldots(n+4)(n+2)},$$

$$m > n. \tag{4}$$

In (4) the numerator is 1 for m = n + 2, for m = n + 4 it is (n + 3), and so on.

We first prove (3) by induction. Since $P_1(x) = x$, and $P_{n+1}(x)$ is orthogonal over (-1, 1) to $P_0(x) = 1$, (3) is true for m = 1. Assume (3) is true for any odd value of m less than n, and use the recurrent relation for the Legendre polynomials,

$$P_{m+2}(x) = \left(\frac{2m+3}{m+2}\right) x\, P_{m+1}(x) - \left(\frac{m+1}{m+2}\right) P_m(x), \tag{5}$$

to obtain

$$\int_{-1}^{1} x^{-1}\, P_{n+1}(x)\, P_{m+2}(x)\, dx = \left(\frac{2m+3}{m+2}\right)\int_{-1}^{1} P_{n+1}(x)\, P_{m+1}(x)\, dx$$

$$- \left(\frac{m+1}{m+2}\right)\int_{-1}^{1} x^{-1}\, P_{n+1}(x)\, P_m(x)\, dx = 0 \tag{6}$$

because of the orthogonality of $P_{n+1}(x)$ and $P_{m+1}(x)$, $m < n$. Hence by induction (3) is true for all odd values of m less than n + 2.

For m = n the normalization integral

$$\int_{-1}^{1} [P_{n+1}(x)]^2 \, dx = 2/(2n + 3) \tag{7}$$

when substituted into (6) leads to

$$\int_{-1}^{1} x^{-1} P_{n+1}(x) P_{n+2}(x) \, dx = 2/(n + 2), \tag{8}$$

as in (4). For m > n, repeated use of (5) and the orthogonality of the Legendre polynomials generates (4) from (8).

We prove (1) by induction. It is obviously true for n = 1. Assume it true for any odd integer n. By (5), (3), and (7),

$$(n + 2)^2 \int_{-1}^{1} x^{-2} [P_{n+2}(x)]^2 \, dx = (2n + 3)^2 \int_{-1}^{1} [P_{n+1}(x)]^2 \, dx$$

$$- 2(2n + 3)(n + 1) \int_{-1}^{1} x^{-1} P_{n+1}(x) P_n(x) \, dx$$

$$+ (n + 1)^2 \int_{-1}^{1} x^{-2} [P_n(x)]^2 \, dx =$$

$$2(2n + 3) + 2(n + 1)^2 = 2(n + 2)^2,$$

whence (2) is true also for n + 2, and therefore for all odd values of n.

Equation (2) follows from (1) by repeated substitution of the recurrent relation (5) and use of (3).

Carl W. Helstrom

Department of Applied Physics and
Information Science

University of California, San Diego

La Jolla, California 92037

Footnote

* This research was carried out under NASA Grant No. 05-009-079.

Resolvability of Objects from the Standpoint of Statistical Parameter Estimation

Carl W. Helstrom*

Department of Applied Physics and Information Science

University of California, San Diego

La Jolla, California, 92037

Abstract

The values of the radiance at points of an incoherently radiating object are considered as parameters of the statistical description of the field at the aperture of an observing optical instrument. By means of the Cramér-Rao inequality a lower bound is set to the mean-square errors of unbiased estimates of the radiance values. The errors are shown to increase rapidly when the object is sampled at points separated by less than a conventional resolution interval.

The ability of an optical instrument to resolve details of an object can be evaluated in various ways. All of them lead to the general conclusion that if the instrument takes in light of wavelength λ from the object through an aperture of diameter a, it will blur details having an angular subtense smaller than λ/a--a conclusion that might be drawn from the undular nature of light simply by dimensional analysis.

A common explanation of how the optical instrument obliterates fine details views it as a linear spatial filter transforming the light field at the object plane into the light field at the image plane. The aperture limits the spatial bandpass of this filter, and the loss of high spatial frequencies prevents the reconstruction of features of inversely proportional dimensions in the object. This viewpoint has led to the proposal that the finite size of the object and the resultant analyticity of its spatial Fourier transform should permit reconstruction of the entire object by mathematical operations on those spatial frequencies that do pass the aperture.[1] The inevitable presence of random background light and the unavoidable introduction of random noise in recording the image light subject any such procedure to deleterious errors.[2] The influence of noise on other linear estimation schemes has been analyzed by Rushforth and Harris.[3]

This approach to resolution through linear filtering is most suitable for coherent object fields. Ordinary objects, however, radiate or reflect incoherent light. Except in microscopy, where coherent illumination may be utilized for the sake of certain phase effects, the light emanating from most objects possesses a very low degree of spatial coherence. With such incoherently illuminated or radiating objects it is not the field of the light that is of interest, for that field is best described as a random process having zero mean value and a most erratic spatio-temporal variation. Rather it is the mean-square value of the field, averaged over many cycles of the dominant temporal frequency Ω, that characterizes the object in the most informative way. Specifically, the mutual coherence function of the light field $\psi_o(\underset{\sim}{u}, t)$ immediately in front of the object has the form

$$\frac{1}{2} \underset{\sim}{E} \psi_o(\underset{\sim}{u}_1, t_1) \psi_o^*(\underset{\sim}{u}_2, t_2) =$$

$$= CB(\underset{\sim}{u}_1) \delta(\underset{\sim}{u}_1 - \underset{\sim}{u}_2) \chi(t_1 - t_2) \exp[-i\Omega(t_1 - t_2)],$$

where $B(\underset{\sim}{u})$ is the radiance of the object at point $\underset{\sim}{u}$, $\chi(\tau)$ is the temporal autocovariance of the field, C is a suitable constant, and $\underset{\sim}{E}$ denotes the statistical expectation. The presence of the two-dimensional delta-function $\delta(\underset{\sim}{u}_1 - \underset{\sim}{u}_2)$ signifies that the coherence length of the light is much smaller than the extent of any details of interest. It is the radiance function $B(\underset{\sim}{u})$ that describes the object for us.

As the light propagates toward the aperture of our optical instrument, its coherence function changes in a predictable fashion,[4] but its field remains a stochastic process, to which is usually added another random field, referred to as the background. This background field has a distribution in frequency and angle that is generally much broader than that of the object light. The values of the radiance $B(\underset{\sim}{u})$ at various points of the object, which are the quantities we really want to know, are related to the net field at the aperture not in a deterministic fashion, but only in a statistical sense. They are *parameters* of the joint probability density functions of the aperture field. The function of the optical instrument is to estimate them by some operation on that field, and the estimates will be subject to error because of the stochastic nature of the light from the background and from the object itself.

In a previous paper we pointed out how the resolvability of details in the object plane might be treated as a problem in decision theory.[5] The optical instrument is required to decide whether two close objects of a specific kind are present, or only one. The probability of its deciding correctly, as a function of the separation of the test objects, measures the resolvability of details having the same size and form.

A subsequent paper introduced a modal expansion of the aperture field arising naturally in an analysis of the detectability of incoherently radiating objects.[6] The strengths of the several modes are directly related to the radiance of the object plane at points separated by a conventional resolution interval $\lambda R/a$, R being the distance of the object. The minimum mean-square errors in unbiased estimates of these radiance values were derived from a quantum-statistical description of the field.

Here we shall develop the statistical theory of resolvability further by viewing the function of an optical instrument as one of estimating the radiance of the object plane. The radiance $B(\underset{\sim}{u})$ is sampled in a suitable manner, and the samples are regarded as parameters of the joint pdf's of the aperture field. By means of the Cramér-Rao inequality lower bounds are set to the mean-square errors of unbiased estimates of those parameters. We shall demonstrate how these minimum mean-square errors soar when the radiance is sampled at points closer together than the conventional resolution interval $\lambda R/a$.

I. Sampling the Object Plane

It is the radiance $B(\underset{\sim}{u})$ of the object plane that is to be estimated as a function of position $\underset{\sim}{u} = (u_x, u_y)$. Since it is impossible to estimate $B(\underset{\sim}{u})$ at all points of the plane, the plane must be sampled, and there are several ways by which this can be done.

The most definitive methods employ a set of functions $F_{\underset{\sim}{m}}(\underset{\sim}{u})$ that are orthogonal over some part O of the object plane, or over the whole of it,

$$\int_0 F_{\underset{\sim}{m}}(\underset{\sim}{u})\, F_{\underset{\sim}{n}}{}^*(\underset{\sim}{u})\, d^2\underset{\sim}{u} = C_{\underset{\sim}{m}}\, \delta_{\underset{\sim}{m}\underset{\sim}{n}}, \tag{1.1}$$

where $C_{\underset{\sim}{m}}$ is a suitable normalization constant. The functions are distinguished by a two-vector index $\underset{\sim}{m} = (m_x, m_y)$. In terms of them the object radiance is written

$$B(\underset{\sim}{u}) = \sum_{\underset{\sim}{m}} B_{\underset{\sim}{m}}\, F_{\underset{\sim}{m}}(\underset{\sim}{u}), \tag{1.2}$$

and in general only a finite number of coefficients, or "samples", $B_{\underset{\sim}{m}}$ will be estimated. The sampling functions $F_{\underset{\sim}{m}}(\underset{\sim}{u})$ are taken dimensionless so that the samples $B_{\underset{\sim}{m}}$ have the dimensions of radiance.

The functions $F_{\underset{\sim}{m}}(\underset{\sim}{u})$ might conveniently be the indicator functions of contiguous rectangles $\Delta_x \times \Delta_y$ in the plane,

$$F_{\underset{\sim}{m}}(\underset{\sim}{u}) = 1, \quad \begin{cases} (m_x - \frac{1}{2})\Delta_x < u_x < (m_x + \frac{1}{2})\Delta_x, \\ \\ (m_y - \frac{1}{2})\Delta_y < u_y < (m_y + \frac{1}{2})\Delta_y \end{cases} \tag{1.3}$$

$$F_{\underset{\sim}{m}}(\underset{\sim}{u}) = 0, \quad \underset{\sim}{u} \text{ elsewhere.}$$

$B_{\underset{\sim}{m}}$ is then the average radiance over the rectangle centered at $(m_x \Delta_x, m_y \Delta_y)$.

Alternatively we might use the sampling functions

$$F_{\underset{\sim}{m}}(\underset{\sim}{u}) = \mathrm{sinc}(x\Delta_x^{-1} - m_x)\ \mathrm{sinc}(y\Delta_y^{-1} - m_y), \tag{1.4}$$

with sinc $z = (\sin\pi z)/\pi z$. If the radiance $B(\underset{\sim}{u})$ has a spatial Fourier transform lying entirely within a rectangle $\Delta_x^{-1} \times \Delta_y^{-1}$ in the spatial-frequency plane, the coefficients in Eq. (1.2) are samples of $B(\underset{\sim}{u})$ at the lattice points,

$$B_{\underset{\sim}{m}} = B(m_x\,\Delta_x,\ m_y\,\Delta_y), \tag{1.5}$$

by the two-dimensional version of the Whittaker-Shannon sampling theorem.[7]

Because the functions $F_{\underset{\sim}{m}}(\underset{\sim}{u})$ in Eqs. (1.3) and (1.4) are centered at points of a lattice, we refer to these forms of sampling as lattice sampling. For both, $C_{\underset{\sim}{m}} = \Delta_x\,\Delta_y = A_\Delta$. The region O is the entire object plane, although in practice only a finite number of samples $B_{\underset{\sim}{m}}$ will be estimated. The smaller Δ_x and Δ_y, the finer the details in the object plane that can be described by Eq. (1.2).

A third representation of the radiance of the object plane can be obtained from a Fourier series, with

$$F_{\underset{\sim}{m}}(\underset{\sim}{u}) = \exp[2\pi i(m_x\,xb_x^{-1} + m_y\,yb_y^{-1})],$$

$$-\frac{1}{2}\,b_x < x < \frac{1}{2}\,b_x,\ -\frac{1}{2}\,b_y < y < \frac{1}{2}\,b_y, \tag{1.6}$$

The region O is now a rectangle $b_x \times b_y$ with area $A_o = b_x\,b_y$, and $C_{\underset{\sim}{m}} = A_o$. The greater the number of terms retained in Eq. (1.2), the finer the detail it can describe. We call this "Fourier sampling".

II. The Aperture Field

The object plane radiates incoherently, creating at the aperture of the optical system a field $\psi_s(\underset{\sim}{r}, t)$--assumed for simplicity to be a scalar--that is a circular-complex gaussian spatio-temporal random process.[8] The probability density functions of this process are completely determined by the mutual coherence function of the object field,

$$\varphi_s(\underset{\sim}{r}_1, t_1; \underset{\sim}{r}_2, t_2) = \underset{\sim}{E}[\psi_s(\underset{\sim}{r}_1, t_1) \psi_s^*(\underset{\sim}{r}_2, t_2)]. \tag{2.1}$$

Also present is background light whose field $\psi_n(\underset{\sim}{r}, t)$ has the same statistical character, but is spatially and temporally white with spectral density N. On the basis of the total aperture field

$$\psi_+(\underset{\sim}{r}, t) = \psi_s(\underset{\sim}{r}, t) + \psi_n(\underset{\sim}{r}, t) \tag{2.2}$$

observed during a finite interval $(0, T)$, the samples $B_{\underset{\sim}{m}}$ of the object radiance are to be estimated.

For convenience of discussion we assume that the object light is quasi-monochromatic and spectrally pure, so that its mutual coherence function can be factored into spatial and temporal parts,[4]

$$\varphi_s(\underset{\sim}{r}_1, t_1; \underset{\sim}{r}_2, t_2) = \varphi_s(\underset{\sim}{r}_1, \underset{\sim}{r}_2)\, \chi(t_1 - t_2) \times \exp[-i\Omega(t_1 - t_2)], \tag{2.3}$$

where $\Omega = 2\pi c/\lambda$ is the central angular frequency of the object light and λ is its wavelength.

The temporal autocovariance function $\chi(\tau)$ is normalized so that $\chi(0) = 1$. Its Fourier transform

$$X(\omega) = \int_{-\infty}^{\infty} \chi(\tau)\, e^{i\omega\tau}\, d\tau, \tag{2.4}$$

which is positive and real, represents the spectral density of the object light, with angular frequencies ω referred to Ω as origin. The bandwidth W of the object light is conveniently defined by

$$W = \left[\int_{-\infty}^{\infty} X(\omega)\, d\omega/2\pi\right]^2 \Big/ \int_{-\infty}^{\infty} [X(\omega)]^2\, d\omega/2\pi$$

$$= |\chi(0)|^2 \Big/ \int_{-\infty}^{\infty} |\chi(\tau)|^2\, d\tau. \tag{2.5}$$

In optics the product WT is normally much greater than 1; indeed, it may be 10^5 or more.

The spatial autocovariance function $\varphi_s(\underset{\sim}{r}_1, \underset{\sim}{r}_2)$ is so normalized that $\varphi_s(\underset{\sim}{r}, \underset{\sim}{r})/2\Omega^2 c$ is the illuminance at point $\underset{\sim}{r}$ of the aperture. The total energy E_s received from the object during the observation interval (0, T) is

$$E_s = T(2\Omega^2 c)^{-1} \int_A \varphi_s(\underset{\sim}{r}, \underset{\sim}{r})\, d^2\underset{\sim}{r}, \tag{2.6}$$

where $\int_A$ indicates an integration over the aperture.

The object plane, we assume, is so far away that the light rays from the part of it being estimated are paraxial. The spatial autocovariance $\varphi_s(\underset{\sim}{r}_1, \underset{\sim}{r}_2)$ can be expressed in terms of the radiance $B(\underset{\sim}{u})$ through the Fresnel-Kirchhoff approximation,[9]

$$\varphi_s(\underset{\sim}{r}_1, \underset{\sim}{r}_2) = (8\pi R^2\Omega^2 c)^{-1} \int_0 B(\underset{\sim}{u})\, \mathcal{E}(\underset{\sim}{r}_1, \underset{\sim}{u})\, \mathcal{E}^*(\underset{\sim}{r}_2, \underset{\sim}{u})\, d^2\underset{\sim}{u},$$

$$\mathcal{E}(\underset{\sim}{r}, \underset{\sim}{u}) = \exp\left(\frac{ik}{2R}|\underset{\sim}{r} - \underset{\sim}{u}|^2\right), \tag{2.7}$$

where $k = \Omega/c = 2\pi/\lambda$ and R is the distance between object and aperture planes. Through Eq. (1.2) the spatial autocovariance function depends on the set $\underset{\sim}{B} = \{B_{\underset{\sim}{m}}\}$ of radiance samples,

$$\varphi_s(\underset{\sim}{r}_1, \underset{\sim}{r}_2; \underset{\sim}{B}) = (8\pi R^2\Omega^2 c)^{-1} \sum_{\underset{\sim}{m}} B_{\underset{\sim}{m}} \int_0 F_{\underset{\sim}{m}}(\underset{\sim}{u})\, \mathcal{E}(\underset{\sim}{r}_1, \underset{\sim}{u})\, \mathcal{E}^*(\underset{\sim}{r}_2, \underset{\sim}{u})\, d^2\underset{\sim}{u}. \tag{2.8}$$

In this way the samples $\underset{\sim}{B} = \{B_{\underset{\sim}{m}}\}$ are parameters of the joint probability density functions of values of the aperture field $\psi_+(\underset{\sim}{r}, t)$ at various points $\underset{\sim}{r}$ and times t.

The foregoing description is based on classical physics and requires $N = K\mathcal{T} >> \hbar\Omega$, where K = Boltzmann's constant, $\mathcal{T}$ is the effective absolute temperature of the background, and $\hbar$ = Planck's constant $h/2\pi$. When $K\mathcal{T} << \hbar\Omega$, the observations are said to be quantum-limited, a condition requiring an easy modification of our results.

III. Errors in Estimates of Radiance Samples

The samples $\underset{\sim}{B} = \{B_{\underset{\sim}{m}}\}$ specifying the radiance distribution of the object plane are to be estimated from observation of the field $\psi_+(\underset{\sim}{r}, t)$ at the aperture of an optical system. The system is to be designed to make the estimates as accurately as possible. How well it can be expected to perform can be assessed by the mean-square errors $\varepsilon_{\underset{\sim}{m}}$ in the estimates $\hat{B}_{\underset{\sim}{m}}$ of the samples $B_{\underset{\sim}{m}}$,

$$\varepsilon_{\underset{\sim}{m}} = \underset{\sim}{E}(\hat{B}_{\underset{\sim}{m}} - B_{\underset{\sim}{m}})^2. \tag{3.1}$$

By restricting ourselves to unbiased estimates,

$$\underset{\sim}{E}(\hat{B}_{\underset{\sim}{m}}) = B_{\underset{\sim}{m}}, \tag{3.2}$$

we can set a lower bound to $\varepsilon_{\underset{\sim}{m}}$ by means of the Cramér-Rao inequality,[10,11]

$$\varepsilon_{\underset{\sim}{m}} = \underset{\sim}{E}(\hat{B}_{\underset{\sim}{m}} - B_{\underset{\sim}{m}})^2 \geq L_{\underset{\sim}{m}\underset{\sim}{m}} \tag{3.3}$$

where the matrix $\underset{\sim}{L} = ||L_{\underset{\sim}{m}\underset{\sim}{n}}|| = \underset{\sim}{H}^{-1}$ is inverse to the matrix $\underset{\sim}{H}$, whose $(\underset{\sim}{m}\underset{\sim}{n})$-element is

$$H_{\underset{\sim}{m}\underset{\sim}{n}} = -\underset{\sim}{E}\left[\frac{\partial^2}{\partial B_{\underset{\sim}{m}} \partial B_{\underset{\sim}{n}}} \ell n\, p(\underset{\sim}{\psi}; \underset{\sim}{B})\right]. \tag{3.4}$$

Here $p(\underset{\sim}{\psi}; \underset{\sim}{B})$ is the joint probability density function of samples $\underset{\sim}{\psi} = \{\psi_+(\underset{\sim}{r}_p, t_q)\}$ of the aperture field at points $\underset{\sim}{r}_p \in A$ and at times $t_q \in (0, T)$. After forming the expectation $\underset{\sim}{E}$, the right-hand side of Eq. (3.4) must be taken to the limit of an infinitely dense sampling of A and (0, T).

The off-diagonal elements of the matrix $\underset{\sim}{L}$ are related to the covariances of unbiased estimates $\hat{B}_{\underset{\sim}{m}}$ at different points. Specifically, if $\underset{\sim}{X}$ is an arbitrary column vector of real elements and $\underset{\sim}{\tilde{X}}$ is its transposed row vector,

$$\underset{\sim}{\tilde{X}}\, \underset{\sim}{V}\, \underset{\sim}{X} \geq \underset{\sim}{\tilde{X}}\, \underset{\sim}{L}\, \underset{\sim}{X}, \tag{3.5}$$

where the elements of the matrix $\underset{\sim}{V} = ||V_{\underset{\sim}{m}\underset{\sim}{n}}||$ are the covariances

$$V_{mn} = E(\hat{B}_m - B_m)(\hat{B}_n - B_n). \tag{3.6}$$

Eq. (3.3) is a special case of Eq. (3.5).

The significance of the multidimensional Cramér-Rao inequality is best understood in terms of the concentration ellipsoid of the errors, a quadric surface whose equation is $\tilde{Y} V^{-1} Y = m + 2$ in an m-dimensional space with coordinates $\tilde{Y} = (y_1, y_2, \ldots, y_m)$, where m is the number of radiance samples.[12] Equivalent to Eq. (3.5) is the inequality

$$\tilde{Y} V^{-1} Y \leq \tilde{Y} H Y, \tag{3.7}$$

which asserts that the concentration ellipsoid lies outside the ellipsoid whose equation is

$$\tilde{Y} H Y = m + 2. \tag{3.8}$$

When the errors are uncorrelated, the axes of the concentration ellipsoid are proportional to their r.m.s. values.

At large signal-to-noise ratio, the maximum-likelihood estimates of the parameters B_m have approximately a joint gaussian distribution, and the level surfaces of this distribution are ellipsoids parallel to the concentration ellipsoid. The Cramér-Rao inequality in this limit becomes asymptotically an equality.[10]

When as here the density functions $p(\psi; B)$ have the circular gaussian form, the elements of the matrix H are given by

$$H_{mn} = \frac{\partial}{\partial B_m^{(1)}} \frac{\partial}{\partial B_n^{(2)}} H(B^{(1)}, B^{(2)}) \Big|_{B^{(1)} = B^{(2)} = B}, \tag{3.9}$$

where the ambiguity function $H(B^{(1)}, B^{(2)})$ is

$$H(B^{(1)}, B^{(2)}) = (E_s/N)^2 (WT)^{-1} \int_A \int_A \varphi_s(r_1, r_2; B^{(1)}) \, \varphi_s(r_2, r_1; B^{(2)}) \, d^2r_1 d^2r_2$$

$$\times \left| \int_A \varphi_S(\underset{\sim}{r}, \underset{\sim}{r}; \underset{\sim}{B})\, d^2\underset{\sim}{r} \right|^{-2}. \tag{3.10}$$

After the differentiations in Eq. (3.9), $\underset{\sim}{B}^{(1)}$ and $\underset{\sim}{B}^{(2)}$ are set equal to the true set $\underset{\sim}{B}$ of radiance samples.[13,14]

If we now substitute from Eqs. (2.7) and (2.8) into Eq. (3.10) and differentiate as in Eq. (3.9), we obtain

$$H_{\underset{\sim}{m}\underset{\sim}{n}} = (E_S/N)^2\ (WT)^{-1}\ B_T^{-2}\ J_{\underset{\sim}{m}\underset{\sim}{n}} \tag{3.11}$$

where

$$B_T = \int_0 B(\underset{\sim}{u})\ d^2\underset{\sim}{u}$$

is the total radiant power of the object plane and

$$J_{\underset{\sim}{m}\underset{\sim}{n}} = \int_0\int_0 F_{\underset{\sim}{m}}(\underset{\sim}{u}_1)\ F_{\underset{\sim}{n}}(\underset{\sim}{u}_2)\ |\mathcal{J}(\underset{\sim}{u}_1 - \underset{\sim}{u}_2)|^2\ d^2\underset{\sim}{u}_1 d^2\underset{\sim}{u}_2 \tag{3.12}$$

with

$$\mathcal{J}(\underset{\sim}{u}) = A^{-1} \int_A I_A(\underset{\sim}{r})\ \exp(-ik\underset{\sim}{r}\cdot\underset{\sim}{u}/R)\ d^2\underset{\sim}{r} \tag{3.13}$$

proportional to the Fourier transform of the indicator function $I_A(\underset{\sim}{r})$ of the aperture.[15] The matrix element $J_{\underset{\sim}{m}\underset{\sim}{n}}$ can also be written

$$J_{\underset{\sim}{m}\underset{\sim}{n}} = A^{-2} \int_A\int_A K_{\underset{\sim}{m}}(\underset{\sim}{r}_1 - \underset{\sim}{r}_2)\ K_{\underset{\sim}{n}}^*(\underset{\sim}{r}_1 - \underset{\sim}{r}_2)\ d^2\underset{\sim}{r}_1 d^2\underset{\sim}{r}_2 \tag{3.14}$$

where

$$K_{\underset{\sim}{m}}(\underset{\sim}{r}) = \int_0 F_{\underset{\sim}{m}}(\underset{\sim}{u})\ \exp\ (ik\underset{\sim}{u}\cdot\underset{\sim}{r}/R)\ d^2\underset{\sim}{u} \tag{3.15}$$

is the Fourier transform of the sampling function $F_{\underset{\sim}{m}}(\underset{\sim}{u})$. In order to evaluate the minimum mean-square errors as in Eq. (3.3) it is necessary to invert the matrix $\underset{\sim}{J} = ||J_{\underset{\sim}{m}\underset{\sim}{n}}||$.

Under quantum-limited conditions, $N = K\mathcal{T} \ll \hbar\Omega$, the factor $(E_s/N)^2 (WT)^{-1}$ in Eq. (3.11) must be replaced by $N_s M f_1(\mathcal{D})$, with[14]

$$f_1(\mathcal{D}) = \mathcal{D}W \int_{-\infty}^{\infty} [X(\omega)]^2 \, [1 + \mathcal{D}WX(\omega)]^{-1} \, d\omega/2\pi, \tag{3.16}$$

where $X(\omega)$ is given by Eq. (2.4), $\mathcal{D} = N_s/\mathcal{N}MWT$, $N_s = E_s/\hbar\Omega$ is the average total number of photons received from the object during the interval $(0, T)$, M is the number of spatial degrees of freedom in the object light at the aperture, and

$$\mathcal{N} = [\exp(\hbar\Omega/K\mathcal{T}) - 1]^{-1}. \tag{3.17}$$

The number M is given by

$$M = \left[\int_A \varphi_s(\underset{\sim}{r}, \underset{\sim}{r};\, \underset{\sim}{B}) \, d^2\underset{\sim}{r} \right]^2 \times \left[\int_A \int_A |\varphi_s(\underset{\sim}{r}_1, \underset{\sim}{r}_2 ;\, \underset{\sim}{B})|^2 \, d^2\underset{\sim}{r}_1 d^2\underset{\sim}{r}_2 \right]^{-1} \tag{3.18}$$

and is roughly equal to AA_o/λ^2R^2, where A is the area of the aperture and A_o is the area of the part of the object plane whose radiance is being estimated. When $\mathcal{D} \gg 1$, an extreme quantum-limited condition, $f_1(\mathcal{D}) \doteq 1$ and the factor $(E_s/N)^2 (WT)^{-1}$ in Eq. (3.11) is replaced by $N_s M$.

IV. Lattice Sampling

Under lattice sampling the functions $F_{\underset{\sim}{m}}(\underset{\sim}{u})$ are obtained by translation of the central function $F_0(\underset{\sim}{u})$,

$$F_{\underset{\sim}{m}}(\underset{\sim}{u}) = F_0(u_x + m_x\,\Delta_x,\, u_y + m_y\,\Delta_y). \tag{4.1}$$

The matrices $\underset{\sim}{H}$ and $\underset{\sim}{J}$ then have the Toeplitz form; that is, their elements depend only on the differences of their indices, $J_{\underset{\sim}{m}\underset{\sim}{n}} = J_{\underset{\sim}{m}-\underset{\sim}{n}}$, where

$$J_{\underset{\sim}{p}} = \int_0\!\!\int_0 F_0(\underset{\sim}{v}_1)\; F_0^*(\underset{\sim}{v}_2)\;|\mathcal{G}(\underset{\sim}{v}_1 - \underset{\sim}{v}_2 - \underset{\sim}{\Delta}_{\underset{\sim}{p}})|^2\; d^2\underset{\sim}{v}_1 d^2\underset{\sim}{v}_2$$

$$= A^{-2}\int_A\!\!\int_A |K_0(\underset{\sim}{r}_1 - \underset{\sim}{r}_2)|^2 \exp[-ik\underset{\sim}{\Delta}_{\underset{\sim}{p}}\cdot(\underset{\sim}{r}_1 - \underset{\sim}{r}_2)/R]\; d^2\underset{\sim}{r}_1 d^2\underset{\sim}{r}_2,$$

$$\underset{\sim}{\Delta}_{\underset{\sim}{p}} = (p_x\,\Delta_x,\, p_y\,\Delta_y). \tag{4.2}$$

In practice the matrix $\underset{\sim}{J} = ||J_{\underset{\sim}{m}-\underset{\sim}{n}}||$ will be finite, and there will be no simple analytical form for its inverse. Under certain conditions, however, an approximate formula for the elements of the inverse matrix $\underset{\sim}{G} = \underset{\sim}{J}^{-1}$ can be obtained by assuming that $\underset{\sim}{J}$ is infinite in extent. We denote this infinite extension of $\underset{\sim}{J}$ by $\underset{\sim}{J}^{\infty}$. Its inverse $\underset{\sim}{G}^{\infty}$ also has the Toeplitz form, and the elements of $\underset{\sim}{G}^{\infty}$ are solutions of the array of simultaneous equations

$$\sum_{\underset{\sim}{q}} G^{\infty}_{\underset{\sim}{p}-\underset{\sim}{q}}\, J^{\infty}_{\underset{\sim}{q}-\underset{\sim}{m}} = \delta_{\underset{\sim}{p}\underset{\sim}{m}}\,. \tag{4.3}$$

These equations can be solved by a Fourier transformation, provided the inverse of $\underset{\sim}{J}^{\infty}$ exists. The diagonal elements $G^{\infty}_{\underset{\sim}{m}}$ of $\underset{\sim}{G}^{\infty}$ will be good approximations to the diagonal elements of $\underset{\sim}{G}$ when $\underset{\sim}{G}$ has many elements, that is, when the diameter of the part 0 of the object plane being estimated is many times greater than the sampling intervals Δ_x and Δ_y. When Δ_x and Δ_y are too small, as we shall see, the approximation breaks down because $\underset{\sim}{J}^{\infty-1}$ no longer exists.

We define the discrete Fourier transforms

$$g(\underset{\sim}{\omega}) = \sum_{\underset{\sim}{p}} G^{\infty}_{\underset{\sim}{p}} \exp(i\underset{\sim}{p}\cdot\omega), \tag{4.4}$$

$$j(\underset{\sim}{\omega}) = \sum_{\underset{\sim}{p}} J^{\infty}_{\underset{\sim}{p}} \exp(i\underset{\sim}{p}\cdot\omega), \tag{4.5}$$

which have periods 2π in ω_x and ω_y. Then, as in the convolution theorem, Eq. (4.3) is equivalent to

$$g(\underset{\sim}{\omega})\ j(\underset{\sim}{\omega}) = 1, \tag{4.6}$$

and the diagonal elements of $\underset{\sim}{G}^{\infty}$ are

$$G^{\infty}_{0} = \int_{-\pi}^{\pi}\int_{-\pi}^{\pi} [j(\omega)]^{-1}\ d^2\underset{\sim}{\omega}/(2\pi)^2. \tag{4.7}$$

The lower bound on the mean-square error $\varepsilon_{\underset{\sim}{m}}$ of an unbiased estimate of $B_{\underset{\sim}{m}}$ is then approximately

$$\varepsilon_{\underset{\sim}{m}} \gtrsim (N/E_s)^2\ WT\ B_T^{\ 2}\ G^{\infty}_{0}. \tag{4.8}$$

The factor G^{∞}_{0} in the right-hand side of this inequality is actually larger than the factor $G_{\underset{\sim}{m}\underset{\sim}{m}} = (\underset{\sim}{J}^{-1})_{\underset{\sim}{m}\underset{\sim}{m}}$ that should appear there, and Eq. (4.8) therefore does not constitute a true lower bound.

Substituting the second part of Eq. (4.2) into Eq. (4.5), we obtain

$$j(\underset{\sim}{\omega}) = A_{\gamma}\ A^{-2} \int_A\int_A \sum_{\underset{\sim}{m}} |K_0(\underset{\sim}{r}_1 - \underset{\sim}{r}_2)|^2$$

$$\times\ \delta(x_1 - x_2 + \gamma_x(m_x - \omega_x/2\pi))\ \delta(y_1 - y_2 + \gamma_y(m_y - \omega_y/2\pi))\ dx_1dy_1dx_2dy_2,$$

$$\gamma_x = \lambda R/\Delta_x,\quad \gamma_y = \lambda R/\Delta_y,\quad A_{\gamma} = \gamma_x\ \gamma_y, \tag{4.9}$$

where m_x and m_y are integers, $\underset{\sim}{m} = (m_x, m_y)$, and $\underset{\sim}{r}_j = (x_j, y_j)$, $j = 1, 2$. Taking the aperture A to be rectangular with sides a_x and a_y, we find after integrating over it

$$j(\omega_x, \omega_y) = A_\gamma A^{-2} \sum_{\underset{\sim}{m}} [a_x - \gamma_x |m_x - \omega_x/2\pi|]$$

$$\times [a_y - \gamma_y |m_y - \omega_y/2\pi|] \; |K_0(\gamma_x(m_x - \omega_x/2\pi), \gamma_y(m_y - \omega_y/2\pi))|^2, \quad (4.10)$$

a term of the sum being set equal to zero whenever either of its square-bracketed factors is negative.

The inverse $[j(\underset{\sim}{\omega})]^{-1}$ ceases to exist when

$$\gamma_x = \lambda R/\Delta_x > 2a_x$$

or

$$\gamma_y = \lambda R/\Delta_y > 2a_y,$$

that is, when $\Delta_x < \lambda R/2a_x = \frac{1}{2}\delta_x$ or $\Delta_y < \lambda R/2a_y = \frac{1}{2}\delta_y$, for then $j(\underset{\sim}{\omega})$ vanishes over a finite area of the rectangle $-\pi < (\omega_x, \omega_y) < \pi$. The infinite form of $\underset{\sim}{J}$ no longer has as inverse, and the diagonal elements of $\underset{\sim}{G}$ cannot be approximated by Eq. (4.7).

Sinc-function Sampling

The analysis is simplest for sinc-function sampling as in Eq. (1.4). From Eq. (3.15),

$$K_0(\underset{\sim}{r}) = A_\Delta = \Delta_x \Delta_y, \quad -\frac{1}{2}\gamma_x < x < \frac{1}{2}\gamma_x, \ -\frac{1}{2}\gamma_y < y < \frac{1}{2}\gamma_y, \tag{4.11}$$

$$K_0(\underset{\sim}{r}) = 0 \text{ elsewhere.}$$

Putting this into Eq. (4.10) we find

$$j(\underset{\sim}{\omega}) = A_\delta A_\Delta [1 - \delta_x|\omega_x|/2\pi\Delta_x] \, [1 - \delta_y|\omega_y|/2\pi\Delta_y],$$

$$A_\delta = \delta_x \delta_y, \tag{4.12}$$

the square-bracketed expressions again vanishing when their contents are negative. Substituting this into Eq. (4.7), we obtain

$$G_0^\infty = 4A_\delta^{-2} \, \ell n(1 - \frac{\delta x}{2\Delta_x}) \, \ell n(1 - \frac{\delta y}{2\Delta_y}),$$

$$\Delta_x > \frac{1}{2}\delta_x, \quad \Delta_y > \frac{1}{2}\delta_y. \tag{4.13}$$

The relative mean-square error in an unbiased estimate of the radiance $B_{\underset{\sim}{m}}$ at point $\underset{\sim}{\Delta_m} = (m_x \Delta_x, m_y \Delta_y)$ is now, by Eq. (4.8),

$$\varepsilon_{\underset{\sim}{m}}/B_{\underset{\sim}{m}}^{\,2} \gtrsim (N/E_\Delta)^2 \, WT(A_\Delta^{\,2}/A_\delta^{\,2}) \, \ell n(1 - \frac{\delta_x}{2\Delta_x}) \, \ell n(1 - \frac{\delta_y}{2\Delta_y})$$

$$= (N/E_\Delta)^2 \, WT \, (A_\Delta/A_\delta) \, G_0'^{\infty}, \tag{4.14}$$

with

$$G_0'^{\infty} = 4(A_\Delta/A_\delta) \, \ell n(1 - \frac{\delta_x}{2\Delta_x}) \, \ell n(1 - \frac{\delta_y}{2\Delta_y}) \tag{4.15}$$

In Eq. (4.14) E_Δ is the total energy that would be received from the area $A_\Delta = \Delta_x \Delta_y$ of the object if it radiated uniformly. The bound is approximately valid only when $\Delta_x > \frac{1}{2}\delta_x$ and $\Delta_y > \frac{1}{2}\delta_y$, where

$$\delta_x = \lambda R/a_x, \quad \delta_y = \lambda R/a_y \tag{4.16}$$

are the conventional resolution elements in the x- and y-directions on the object plane.

When the sampling intervals Δ_x and Δ_y are much greater than the resolution elements δ_x and δ_y, respectively, the relative mean-square error in Eq. (4.14) becomes approximately

$$\varepsilon_{\underset{\sim}{m}}/B_{\underset{\sim}{m}}^2 \gtrsim (N/E_s)^2 \text{ (MWT) } M_\Delta \tag{4.17}$$

where M_Δ is the number of sampling rectangles into which the object is divided, $E_s = M_\Delta E_\Delta$ is the total energy received from the object, and

$$M = A_o/A_\delta = M_\Delta A_\Delta/A_\delta \tag{4.18}$$

is the number of spatial degrees of freedom in the object field. Since the total radiant power B_T is proportional to the sum

$$\sum_{\underset{\sim}{m}} B_{\underset{\sim}{m}},$$

which contains M_Δ terms, we conclude that the relative mean-square error in an estimate of B_T is bounded by

$$\underset{\sim}{E}(\hat{B}_T - B_T)^2/B_T^2 \gtrsim (N/E_s)^2 \text{ MWT}, \tag{4.19}$$

in agreement with a previous result.[17]

With sinc-function sampling the matrix elements $J_{\underset{\sim}{p}}$ themselves can be evaluated in closed form from Eqs. (4.2) and (4.11). They are

$$J_{\underset{\sim}{p}} = A_\delta A_\Delta J_{\underset{\sim}{p}}' \tag{4.20}$$

with

$$J_{\underset{\sim}{p}}' = (A_\Delta/A_\delta) \operatorname{sinc}^2(p_x \Delta_x/\delta_x) \operatorname{sinc}^2(p_y \Delta_y/\delta_y), \qquad \Delta_x \le \tfrac{1}{2}\delta_x, \; \Delta_y \le \tfrac{1}{2}\delta_y, \tag{4.21}$$

and

$$\begin{aligned} J_{\underset{\sim}{p}}' &= (2\pi^2)^{-2} (A_\delta/A_\Delta) \left[1 - (-1)^{p_x}\right] \left[1 - (-1)^{p_y}\right]/p_x^2 p_y^2, \\ J_{\underset{\sim}{0}}' &= \left(1 - \frac{\delta_x}{4\Delta_x}\right)\left(1 - \frac{\delta_y}{4\Delta_y}\right), \qquad \Delta_x > \tfrac{1}{2}\delta_x, \; \Delta_y > \tfrac{1}{2}\delta_y. \end{aligned} \tag{4.22}$$

One-Dimensional Object

The accuracy of our approximation to $\underset{\sim}{G}^{\infty}$ can be most easily assessed numerically for estimates of the radiance of a one-dimensional object. We consider the matrix $\underset{\sim}{J}' = ||J'_{m-n}||$ whose elements are the one-dimensional versions of those in Eqs. (4.21), (4.22), which were derived for sinc-function sampling. Here, after subscripts x and y are dropped,

$$J_p' = (2\pi^2)^{-1}\ (\delta/\Delta)\ [1 - (-1)^p]/p^2$$

$$J_0' = (1 - \delta/4\Delta),\quad \Delta > \frac{1}{2}\delta, \tag{4.23}$$

$$J_p' = (\Delta/\delta)\ \mathrm{sinc}^2(p\Delta/\delta),\quad \Delta < \frac{1}{2}\delta. \tag{4.24}$$

Eleven- and fifteen-rowed matrices $||J'_{m-n}||$ were inverted by a digital computer. The central--and largest--element of the inverse matrix $\underset{\sim}{G}'$ is plotted in Fig. 1 as a function of the ratio δ/Δ; these are the curves marked "11" and "15". The curve marked "∞" displays the diagonal elements $G_0'^{\infty}$ of the infinite matrix $\underset{\sim}{J}'^{\infty}$; they are given by the one-dimensional form of Eq. (4.15),

$$G_0'^{\infty} = 2(\Delta/\delta)|\ell n(1 - \delta/2\Delta)|,\quad \delta/\Delta < 2. \tag{4.25}$$

The graph illustrates the extremely rapid increase in the mean-square error when an attempt is made to estimate the radiance at points closer than $\frac{1}{2}\delta = \lambda R/2a$, where a is the width of the aperture. The central element of $\underset{\sim}{J}'^{-1}$ soon reaches astronomical values, rising the faster, the larger the number of points at which the radiance samples are unknown. For $\Delta < \frac{1}{2}\delta$, on the other hand, the minimum mean-square error of the estimate is insensitive to the number of points involved and is close to the value calculated by assuming the number to be infinite.

The diagonal elements of $\underset{\sim}{J}'^{-1}$ decrease from the center to the corners of the matrix. The reason for this is that the assumption of a finite number of sample points requires the radiance to be known precisely at points outside the sampled area. The estimates of B_m for points near the edge are influenced by a smaller number of unknown radiance values and can therefore be made more accurately.

At large signal-to-noise ratio the elements G'_{mn} of the inverse matrix $\underset{\sim}{J}'^{-1}$ are nearly proportional to the covariances of the errors in the estimates B_m and B_n. For $\Delta > \frac{1}{2}\delta$ these are approximately equal to the elements G'^{∞}_{m-n} of $\underset{\sim}{G}'^{\infty}_{0} = \underset{\sim}{J}'^{\infty-1}$, where from Eq. (4.4)

$$G'^{\infty}_{p} = \int_{-\pi}^{\pi} [j'(\omega)]^{-1} \exp(-ip\omega)\ d\omega/2\pi . \tag{4.26}$$

In Table 1 we have listed the asymptotic correlation coefficients $G'^{\infty}_{p}/G'^{\infty}$ for several values of δ/Δ. When Δ is much larger than δ, the estimates are approximately uncorrelated. As Δ increases, the correlation spreads over more and more adjacent elements.

Table 1

Correlation Coefficient of Radiance Estimates

	Number of Intervals, p							
δ/Δ	0	1	2	3	4	5	6	7
0	1.0	0.0	0.0	0.0	0.0	0.0	0.0	0.0
0.5	1.0	-0.0582	0.00417	-0.00676	0.00107	-0.00245	0.00048	-0.00126
1.0	1.0	-0.139	0.0237	-0.0194	0.00658	-0.00720	0.00301	-0.00373
1.5	1.0	-0.269	0.0882	-0.0576	0.0307	-0.0242	0.0152	-0.0131
1.9	1.0	-0.505	0.304	-0.230	0.174	-0.142	0.115	-0.0983
3.0	1.0	-0.936	0.764	-0.538	0.321	-0.155	0.0556	-0.00117

The last line of Table 1 lists the correlation coefficients G'_{p0}/G'_{00} obtained from the central row of the inverse $\underset{\sim}{G}' = \underset{\sim}{J}'^{-1}$ of the 15×15 matrix $\underset{\sim}{J}'$, whose elements were calculated from Eq. (4.24) for $\delta/\Delta = 3$. Adjacent estimates are much more strongly correlated than for $\delta/\Delta < 2$. The small value for $p = 7$ reflects the fact that the two sample points 7 units on each side of center lie at the edge of the observed area, where the estimates are influenced by somewhat fewer unknown radiance values than for points near the center.

Indicator-Function Sampling

When the indicator functions of Eq. (1.3) are used for sampling in one or two dimensions, the matrix elements $J'_{\underset{\sim}{p}}$ are integrals that cannot be expressed in closed form. The Fourier transform of the central indicator function is

$$K_0(\underset{\sim}{r}) = A_\Delta \operatorname{sinc}(x/\gamma_x) \operatorname{sinc}(y/\gamma_y), \tag{4.27}$$

with $\gamma_x = \lambda R/\Delta_x$, $\gamma_y = \lambda R/\Delta_y$. For a one-dimensional object the approximate values of the central diagonal elements of $\underset{\sim}{J}'^{-1}$ are

$$G'^{\infty}_{0} = (\pi^2/\delta) \int_{-1/2}^{1/2} \csc^2(\pi u) \, \{\sum_{m=-\infty}^{\infty} (u - m)^{-2} \, [1 - |u - m| \, \delta/\Delta]\}^{-1} \, du, \qquad \Delta < 2\delta, \tag{4.28}$$

corresponding to Eq. (4.25). This has been plotted as a dashed curve in Fig. 1; numerical integration was required.

V. Fourier Sampling

The minimum mean-square error of an unbiased estimate of any of the coefficients $B_{\underset{\sim}{m}}$ in the expansion of the object radiance, Eq. (1.2), is given by Eqs. (3.3) and (3.9),

$$\varepsilon_{\underset{\sim}{m}} \geq (N/E_S)^2 \; WT \; B_T^2 \; G_{\underset{\sim}{m}\underset{\sim}{m}}, \tag{5.1}$$

where $G_{\underset{\sim}{m}\underset{\sim}{m}}$ is a diagonal element of the matrix $\underset{\sim}{G} = \underset{\sim}{J}^{-1}$. The elements of $\underset{\sim}{J}$ are in turn given by Eq. (3.10). The matrix inversion would be simple if $\underset{\sim}{J}$ were a diagonal matrix, and it is natural to look for the kind of sampling for which it is. The matrix $\underset{\sim}{J}$ will be diagonal if the orthogonal functions $F_{\underset{\sim}{m}}(\underset{\sim}{u})$ are eigenfunctions of the integral equation

$$\lambda_{\underset{\sim}{m}} \, F_{\underset{\sim}{m}}(\underset{\sim}{u}) = \int_0 |\, \mathcal{G}(\underset{\sim}{u} - \underset{\sim}{v})\,|^2 \; F_{\underset{\sim}{m}}(\underset{\sim}{v}) \; d^2\underset{\sim}{v}, \tag{5.2}$$

whose kernel $|\,\mathcal{G}(\underset{\sim}{u} - \underset{\sim}{v})|^2$ is defined by Eq. (3.11).

The object whose radiance is to be estimated is assumed to occupy a finite region 0 of the object plane. Its diameter will in general be much larger than the width of the kernel $|\,\mathcal{G}(\underset{\sim}{u})\,|^2$, which is of the order of $\lambda RA^{-1/2}$, A being the area of the aperture. As discussed previously,[18] the eigenfunctions are then, for a rectangular object, sinusoids as in Eq. (1.6); and the eigenvalues $\lambda_{\underset{\sim}{m}}$, which will be the diagonal elements of $\underset{\sim}{J}$, are the values of the Fourier transform of the kernel $|\,\mathcal{G}(\underset{\sim}{u})\,|^2$ evaluated at points separated in the x- and y-directions by $2\pi/b_x$ and $2\pi/b_y$, respectively, where b_x and b_y are the length and breadth of the object. Thus we are led to Fourier sampling.

The Fourier transform of the kernel $|\,\mathcal{G}(\underset{\sim}{u})\,|^2$ is, by the convolution theorem, the self-convolution of the indicator function $I_A(\underset{\sim}{r})$ of the aperture. For a rectangular aperture $a_x \times a_y$, this is

$$\Phi(\underset{\sim}{\omega}) = \int_{-\infty}^{\infty}\int_{-\infty}^{\infty} |\mathcal{G}(\underset{\sim}{u})|^2 \exp(i\underset{\sim}{\omega}\cdot\underset{\sim}{u})\, d^2\underset{\sim}{u} =$$

$$(\lambda R/A)^2 \int_A I_A(\underset{\sim}{r})\, I_A(k^{-1} R\underset{\sim}{\omega} - \underset{\sim}{r})\, d^2\underset{\sim}{r} =$$

$$(\lambda R/A)^2 \,[a_x - |k^{-1} R\omega_x|]\,[a_y - |k^{-1} R\omega_y|],$$

$$|\omega_x| < ka_x/R,\ |\omega_y| < ka_y/R, \tag{5.3}$$

and $\Phi(\underset{\sim}{\omega}) = 0$ for $\underset{\sim}{\omega}$ outside the rectangle $(ka_x/R) \times (ka_y/R)$. Hence the eigenvalues of Eq. (5.2) are approximately

$$\lambda_{\underset{\sim}{m}} = (\lambda R)^2 \,[1 - |m_x|\, \delta_x/b_x]\,[1 - |m_y|\, \delta_y/b_y]/A,$$

$$\delta_x = \lambda R/a_x << b_x,\quad \delta_y = \lambda R/a_y << b_y, \tag{5.4}$$

with $[x] = 0$ for $x < 0$.

The minimum relative mean-square error of an unbiased estimate of the coefficient

$$B_{\underset{\sim}{m}} = (b_x\, b_y)^{-1} \int_0 B(x, y) \exp 2\pi i(m_x\, xb_x^{-1} + m_y\, yb_y^{-1})\, dxdy \tag{5.5}$$

is

$$\varepsilon_{\underset{\sim}{m}}/B_0^{\,2} \geq (N/E_s)^2\, MWT[1 - |m_x|\, \delta_x/b_x]^{-1}\,[1 - |m_y|\, \delta_y/b_y]^{-1}, \tag{5.6}$$

where $M = AA_o/(\lambda R)^2 = A_o/A_\delta$ is the number of spatial degrees of freedom in the object O. ($A_o = b_x\, b_y$ = the area of the object.) We have referred the mean-square errors to the value of the central coefficient $B_0 = B_T/A_o$. For $\underset{\sim}{m} = \underset{\sim}{0}$ Eq. (5.6) agrees with Eq. (4.19).

As $|m_x|$ and $|m_y|$ increase, so does the minimum relative mean-square error $\varepsilon_{\underset{\sim}{m}}/B_0^{\,2}$. It appears to become infinite for $|m_x| = b_x/\delta_x$ or $|m_y| = b_y/\delta_y$, but the exact eigenvalues $\lambda_{\underset{\sim}{m}}$ do not go to zero at that point, although they become extremely small for $|m_x| > b_x/\delta_x$, $|m_y| > b_y/\delta_y$. The complex exponential sampling function $F_{\underset{\sim}{m}}(\underset{\sim}{u})$ in Eq. (1.6) will bear a significantly large coefficient $B_{\underset{\sim}{m}}$ when the object contains many details whose widths in the x- and y-directions are of the order of b_x/m_x and b_y/m_y, respectively. This coefficient will be subject to a very large error when the details have widths smaller than $\delta_x = \lambda R/a_x$ and $\delta_y = \lambda R/a_y$.

Footnotes

* This research was carried out under NASA Grant No. 05-009-079.

1. H. Wolter, Progress in Optics, E. Wolf, Ed. (North-Holland Publ. Co., Amsterdam) 1, 157 (1961).
2. Y. T. Lo, J. Appl. Phys. 32, 2052 (1961).
3. C. K. Rushforth and R. W. Harris, J. Opt. Soc. Am. 58, 539 (1968).
4. L. Mandel and E. Wolf, Rev. Mod. Phys. 37, 231 (1965).
5. C. W. Helstrom, J. Opt. Soc. Am. 59, 164 (1969).
6. C. W. Helstrom, "The Modal Decomposition of Aperture Fields in the Detection and Estimation of Incoherent Objects", submitted to J. Opt. Soc. Am.
7. D. Gabor, Progress in Optics, E. Wolf, Ed. (North-Holland Publ. Co., Amsterdam) 1, 109 (1961).
8. C. W. Helstrom, Statistical Theory of Signal Detection (Pergamon Press, Ltd., Oxford, 1968) 2nd Ed. See pp. 69-72.
9. Ref. 5, Eqs. (1.8), (1.9).
10. H. Cramér, Mathematical Methods of Statistics (Princeton University Press, 1946), pp. 473 ff.
11. C. R. Rao, Bull. Calcutta Math. Soc. 37, 81 (1945).
12. L. Schmetterer, Mathematische Statistik (Springer-Verlag, New York, 1966), p. 63.
13. Ref. 5, Appendix B.
14. C. W. Helstrom, "Estimation of Object Parameters by a Quantum-Limited Optical System", submitted to J. Opt. Soc. Am.
15. Ref. 1, Eq. (A4).
16. C. W. Helstrom, "Detection of Incoherent Objects by a Quantum-Limited Optical System", J. Opt. Soc. Am. 59, (1969). See Eq. (5.10).

17. Ref. 5, Eq. (6.3), in which $\mathcal{J} = M^{-1/2}$.

18. Ref. 6, Section I. See especially Eqs. (1.15), (1.21).

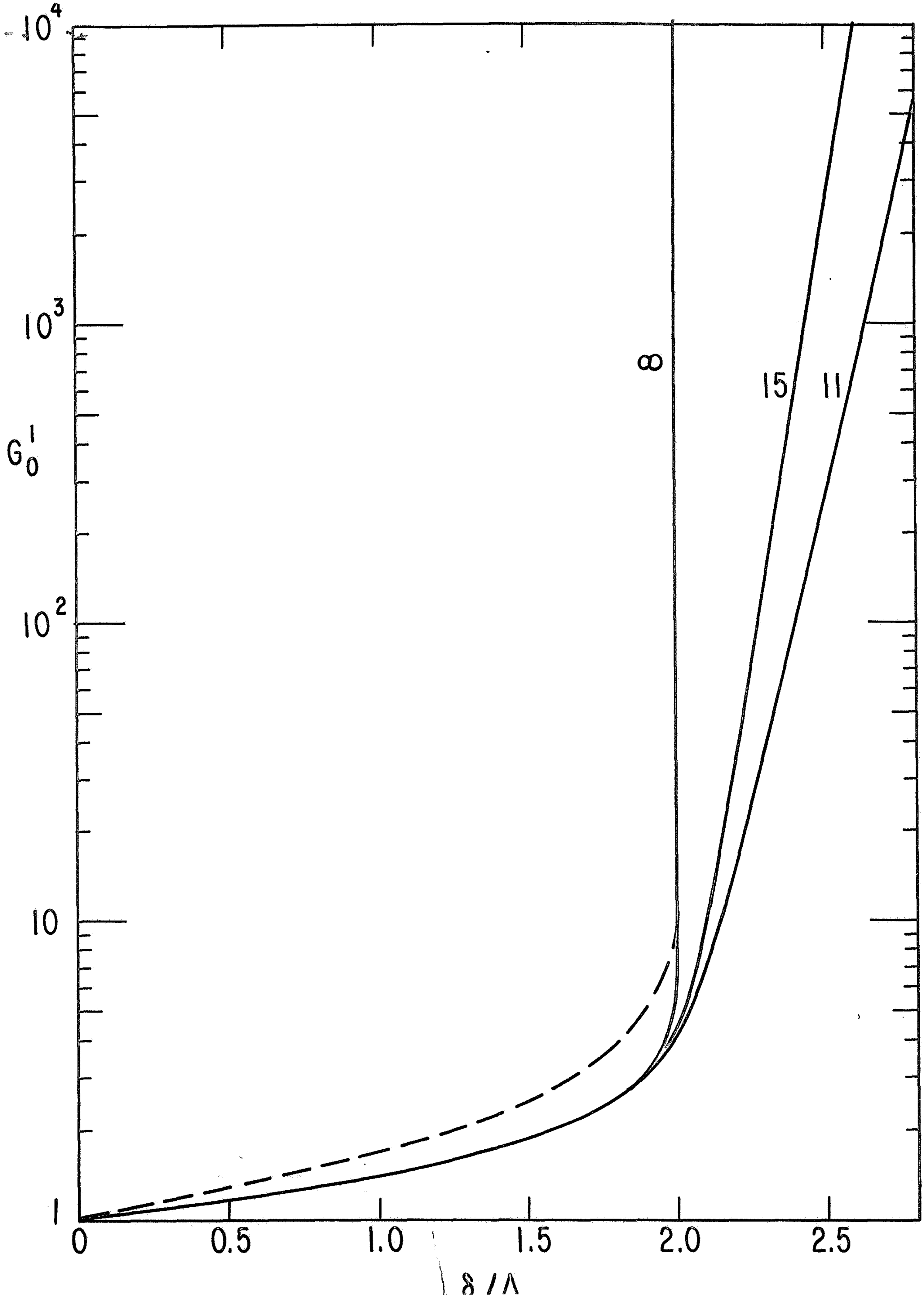

10^4
10^3
10^2
10
1
G_0^1
∞
15
11
0
0.5
1.0
1.5
2.0
2.5
δ / Λ